Consistency of Perfect Fluidity and Jet Quenching in semi-Quark-Gluon Monopole Plasmas

Jiechen Xu
Columbia University

Based on: JX, Jinfeng Liao, Miklos Gyulassy, arXiv:1411.3673
JX, Alessandro Buzzatti, Miklos Gyulassy, JHEP 1408, 063 (2014)

April 17, 2015 @ BNL, Upton, NY

Outline

- Motivation: *the inconsistency between the bulk viscous transport properties controlling the "perfect fluidity" of QGPs and the jet transport properties controlling the hard jet quenching observables at RHIC and LHC*
- Nonperturbative medium near T_c
- Perturbative jet quenching
- CUJET3.0 = pQCD + semi-QGP + magnetic monopoles
- qhat/T^3(T), η/s(T), high-p_T R_{AA} and v_2
- Summary

Bulk perfect fluidity vs pQCD jet quenching

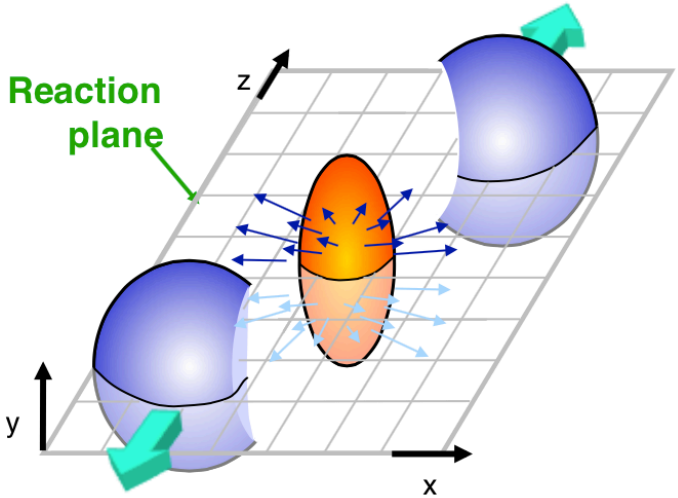

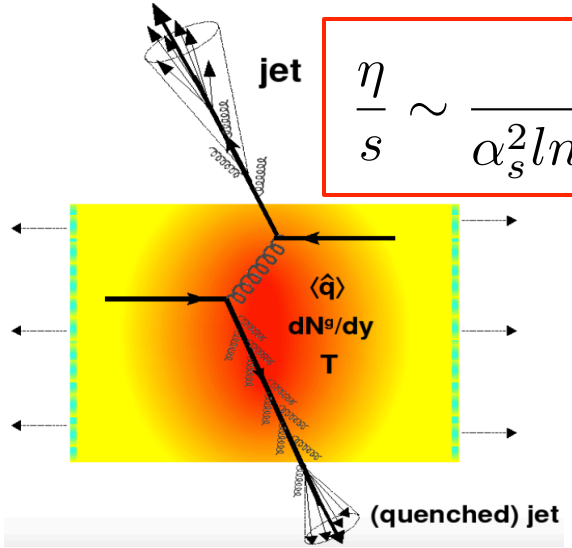

$$\frac{\eta}{s} \sim \frac{1}{\alpha_s^2 ln(\alpha_s^{-1})}$$

Bulk: nonperturbative, η/s~0.1-0.2

Jet quenching: pQCD, η/s~0.5-1.0

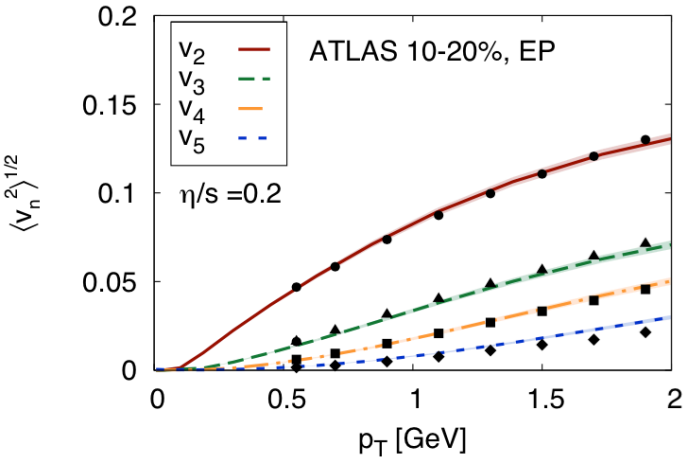

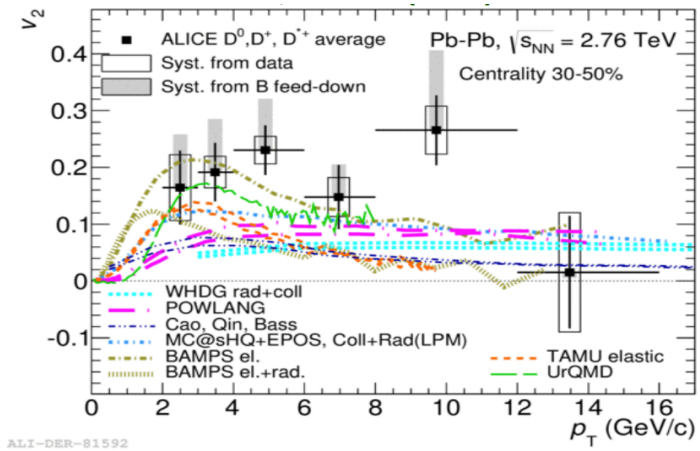

Bulk: IP-Glasma + MUSIC, Gale et al. 2013

Jet quenching: 50% underprediction of high pT v2

❖ Bulk perfect fluidity and jet quenching inconsistent?

Beyond the “standard model” of heavy ion collisions

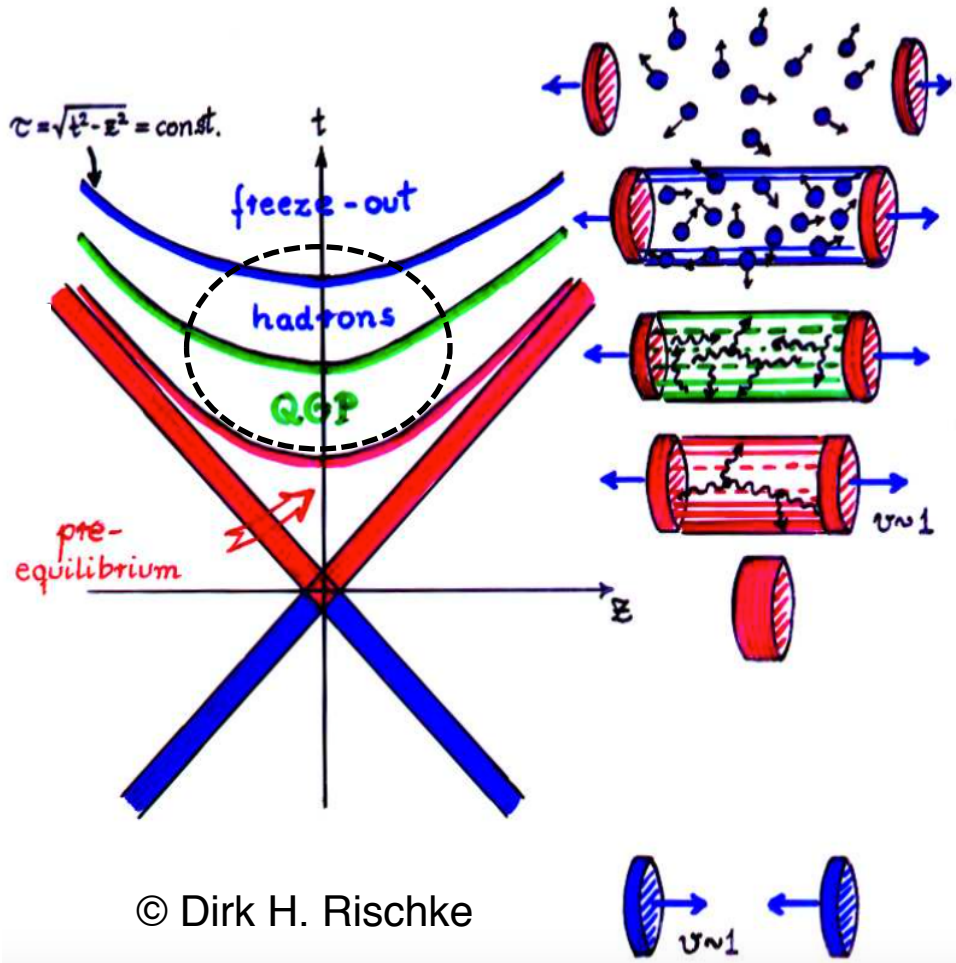

© Dirk H. Rischke

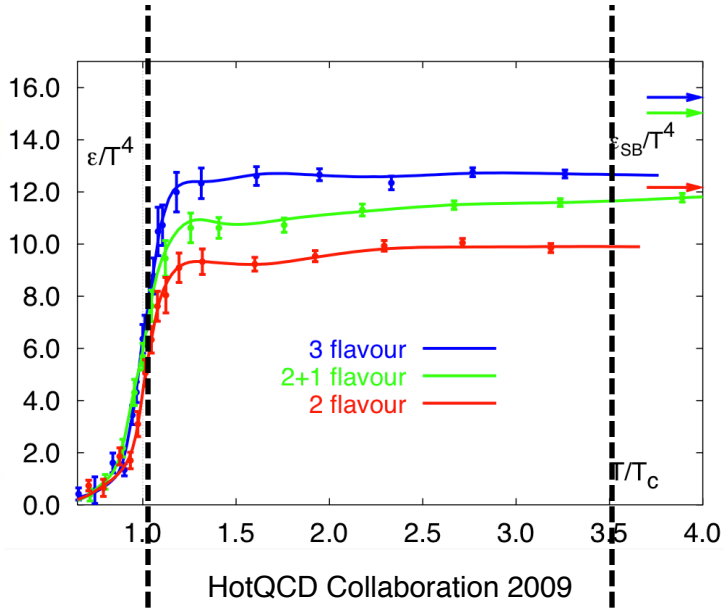

HotQCD Collaboration 2009

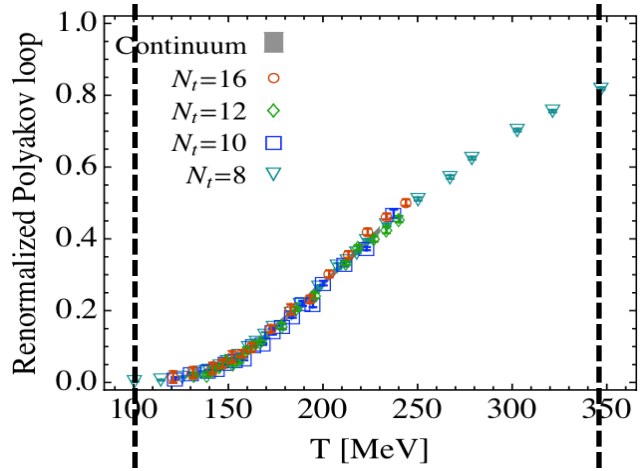

Wuppertal-Budapest 2010

- What would be a lattice compatible, microscopic description of the near Tc matter?
  - Does this help reconciling the “soft” vs “hard” transport inconsistency?

Color confinement: Dual Superconductivity

- Dual superconductivity is a promising mechanism for quark confinement. [Y.Nambu (1974). G.'t Hooft, (1975). S.Mandelstam, (1976) A.M. Polyakov (1975)]

superconductor

- Condensation of electric charges (Cooper pairs)
- Meissner effect: Abrikosov string (magnetic flux tube) connecting monopole and anti-monopole
- Linear potential between monopoles

dual superconductor

- Condensation of magnetic monopoles
- Dual Meissner effect: formation of a hadron string (chromo-electric flux tube) connecting quark and antiquark
- Linear potential between quarks

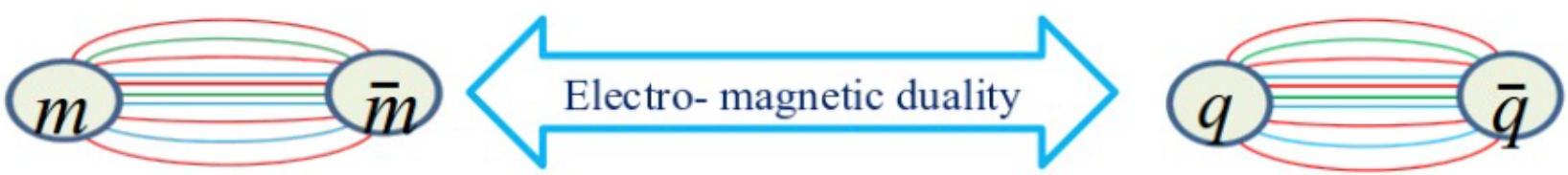

Akihiro, Shibata, Trento 2013

Kondo, Kato, Shibata, Shinohara, arXiv:1409.1599

Liao-Shuryak "E-M See-Saw" Scenario

T<< Lambda_QCD | T ~ Lambda_QCD | T>> Lambda_QCD

Vacuum: confined | Tc | sQGP | ***wQGP: screening*** | T

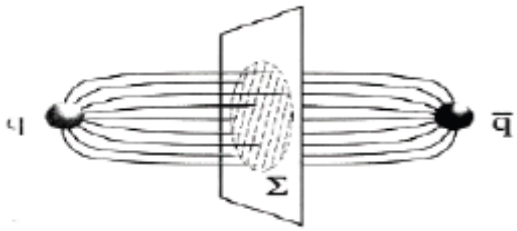

Emergent plasma with E & M charges:
chromo-magnetic monopoles are the "missing DoF"

Plasma of E-charges
E-screening: g T
M-screening: g^2 T

Electric Flux Tube:
Magnetic Condensate

$$\alpha_E * \alpha_M = 1.$$

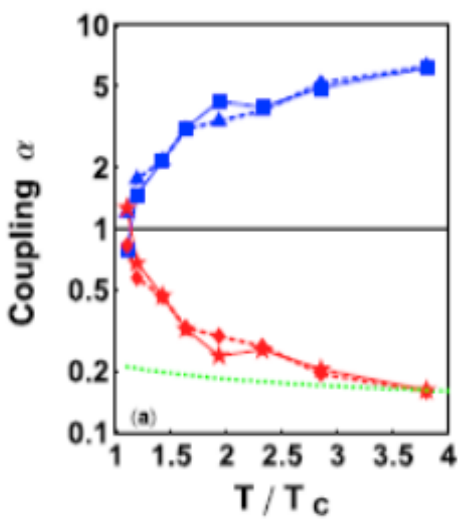

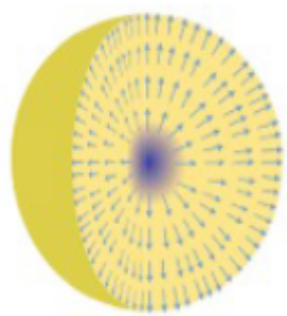

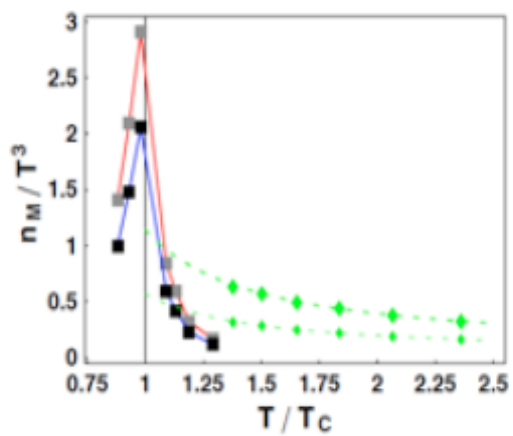

Phys.Rev.C75:054907,2007; Phys.Rev.Lett.101:162302,2008; Phys.Rev.C77:064905,2008; Phys.Rev.D82:094007,2010; Phys.Rev.Lett.109:152001,2012.

❖ Jinfeng Liao, APS DNP Hawaii 2014

The QCD matter near Tc

- Near Tc: semi-QGP (L power suppression of q & g, c.f. Hidaka, Pisarski) + magnetic monopoles = sQGMP?

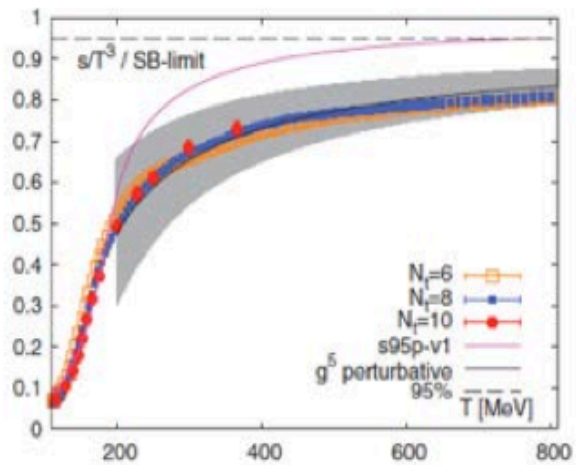

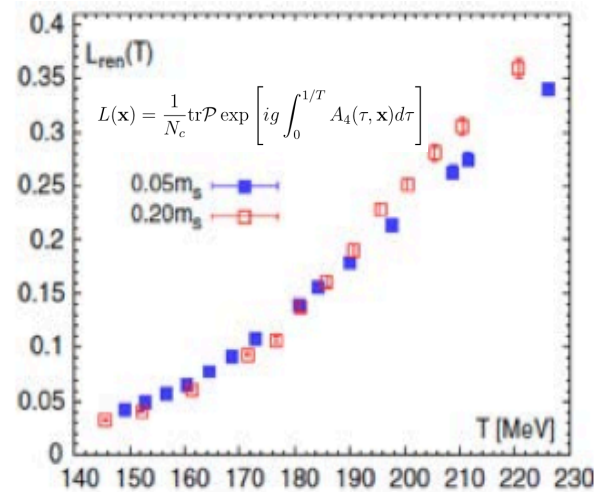

A region around Tc with liberated degrees of freedom

but only partially liberated color-electric objects—missing D.o.F.:

semi-QGP + emergent magnetic component

- Courtesy of Jinfeng Liao

- How can we implement such a microscopic model of QGP in the strong coupling regime into a pQCD jet energy loss framework?
  - Does this explain all the jet quenching data at RHIC and LHC?
  - Does this provide a quantitative connenction between the perfect fluidity of QGP and pQCD jet quenching?

Jet tomography in high energy A+A collisions

- Hard processes happen before the formation of the medium
  - Initial hard parton production rate in AA collisions can be calculated from pQCD

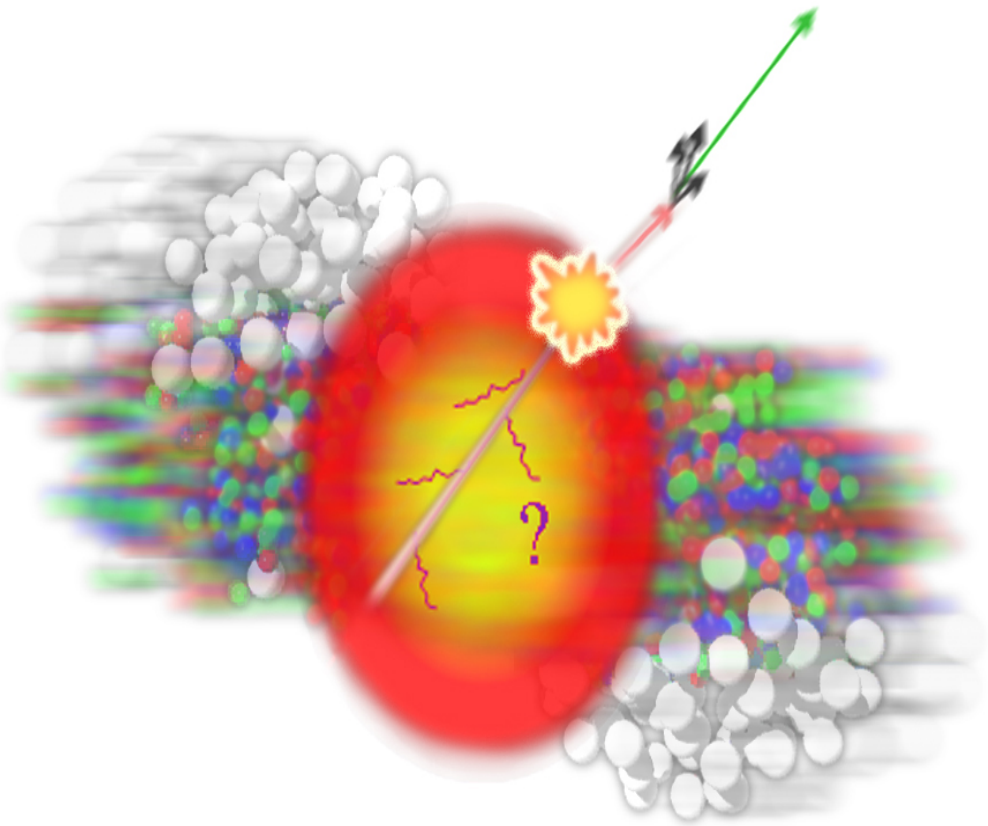

- Quarks and gluons have final state interaction
  - Jets will be modified by interacting with the medium

- Jet tomography: one can use hard jets as probes to study the properties of the medium

pQCD jet quenching

- pQCD jet energy loss models: AMY, ASW, BDMPS-Z, Higher twist, (D)GLV…

- (D)GLV
  - The plasma: well-separated, static, color screened scattering centers
  - Energy loss: expansion in the number of parton-medium scatterings (opacity expansion)
    - Dominated by the first hard contribution. ("Thin plasma")
  - Include interference of "vacuum" radiation, vertex radiation and gluon rescatterings

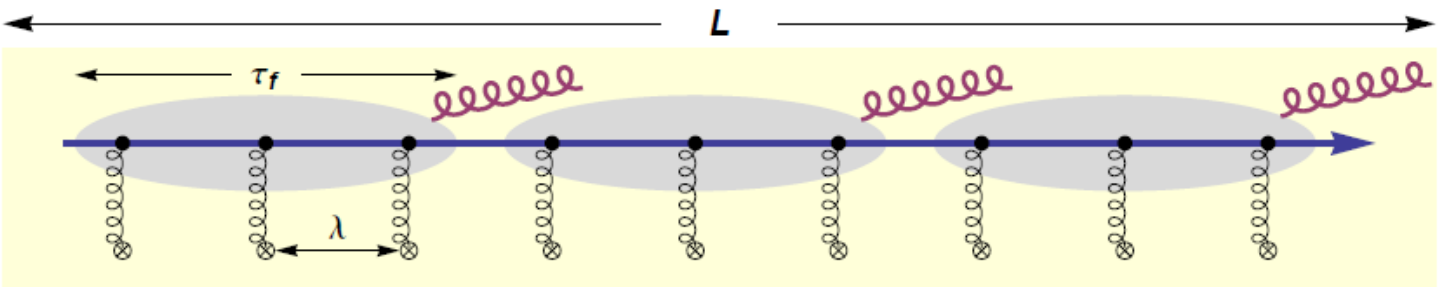

- $\tau_f<\lambda<L$ Incoherent multiple collisions
- $\lambda<\tau_f<L$ LPM effect
- $\lambda<L<\tau_f$ "Factorization" limit

(D)GLV Opacity Expansion

$$x\frac{dN_g^n}{dxd^2\mathbf{k}} = \frac{C_R\alpha_s}{\pi^2}\frac{1}{n!}\left(\frac{L}{\lambda_g}\right)^n \int \prod_{i=1}^{n}\left(d^2\mathbf{q}_i\left(|\bar{v}_i(\mathbf{q}_i)|^2 - \delta^2(\mathbf{q}_i)\right)\right)$$

$$\times\ -2\,\mathbf{C}_{(1\cdots n)}\cdot\sum_{m=1}^{n}\mathbf{B}_{(m+1\cdots n)(m\cdots n)}$$

$$\times\ \left(\cos\left(\sum_{k=2}^{m}\Omega_{(k\cdots n)}\Delta z_k\right) - \cos\left(\sum_{k=1}^{m}\Omega_{(k\cdots n)}\Delta z_k\right)\right)$$

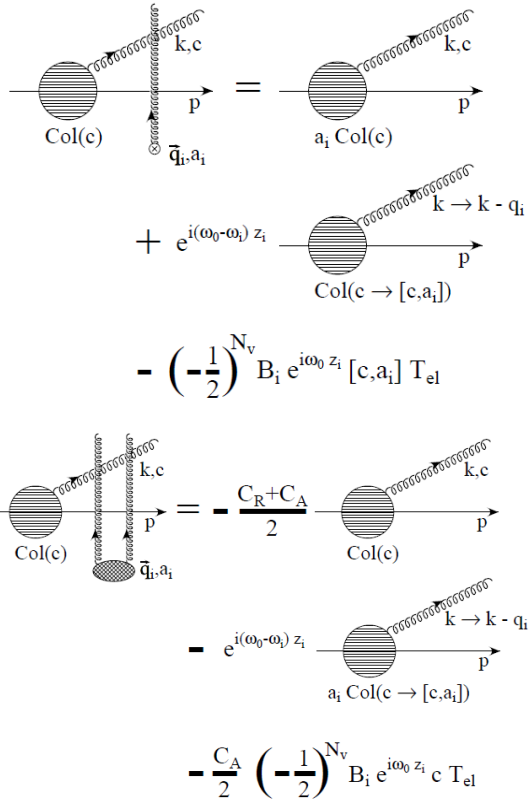

$$\mathbf{C}_{(1\cdots n)} = \frac{\mathbf{k}-\mathbf{q}_1-\cdots-\mathbf{q}_n}{(\mathbf{k}-\mathbf{q}_1-\cdots-\mathbf{q}_n)^2+\chi^2}$$

$$\mathbf{H} = \frac{\mathbf{k}}{\mathbf{k}^2+\chi^2}$$

$$\mathbf{B}_{(i)} = \mathbf{H} - \mathbf{C}_{(i)}$$

$$\mathbf{B}_{(1\cdots m)(1\cdots n)} = \mathbf{C}_{(1\cdots m)} - \mathbf{C}_{(1\cdots n)}$$

$$\Omega_{m\cdots n} = \frac{(\mathbf{k}-\mathbf{q}_m-\cdots-\mathbf{q}_n)^2+\chi^2}{2xE}$$

(Gyulassy, Levai, Vitev, Djordjevic)

$$\chi^2 = M^2x^2 + m_g^2(1-x) \quad m_g = \mu/\sqrt{2}\ ,\ \mu = gT\sqrt{N_c/3+N_f/6}$$

$$|\bar{v}_i(\mathbf{q}_i)|^2 = \frac{{\mu_i}^2}{\pi(\mathbf{q}_i^2+{\mu_i}^2)^2}$$

(Gyulassy-Wang, 1996)

Convergence of the DGLV opacity series

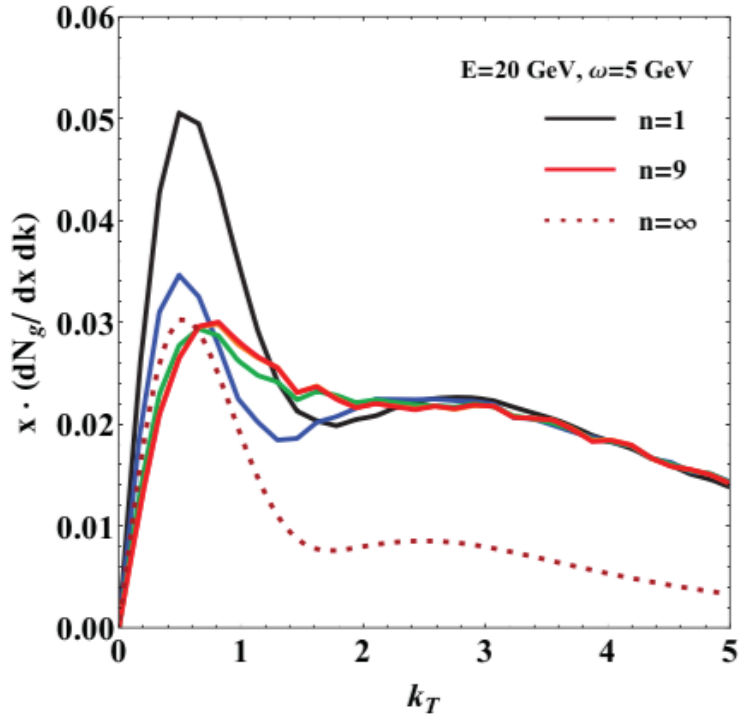

Figure 15. Radiated gluon transverse momentum distribution for a heavy quark jet with energy $E = 20\,\mathrm{GeV}$ traversing a brick plasma of size $L = 5\,\mathrm{fm}$ emitting a gluon with energy $\omega = 5\,\mathrm{GeV}$. The mass of the quark $M = 4.75\,\mathrm{GeV}$. The DGLV opacity series calculated up to n=1 (black), 3 (blue), 5 (green), 7 (orange), 9 (red) are shown in the figure. The opacity expansion computed up to ninth order is shown to converge to the ASW multiple soft scattering limit (maroon, dashed) for small $k_\perp \lesssim \hat{q}L \approx 1\,\mathrm{GeV}$. At large $k_\perp$, differs from the ASW limit, DGLV has a robust Laudau tail. Other parameters used in the simulation are: $\lambda = 1.16\,\mathrm{fm}$, $\mu = 0.5\,\mathrm{GeV}$, $m_g = 0.356\,\mathrm{GeV}$, $T = 0.258\,\mathrm{GeV}$, $n_f = 0$, $\alpha_s = 0.3$.

JX, Buzzatti, Gyulassy, JHEP 1408, 063 (2014)

The heavy quark energy loss puzzle
& The surprising transparency of QGP at LHC

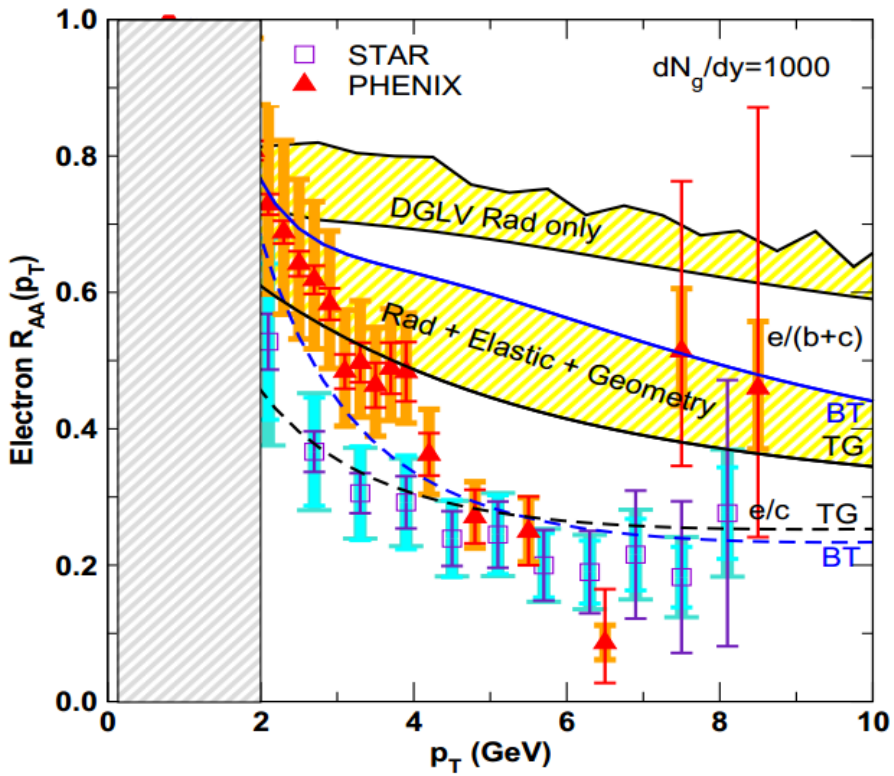

WHDG, NPA784,426(2007)

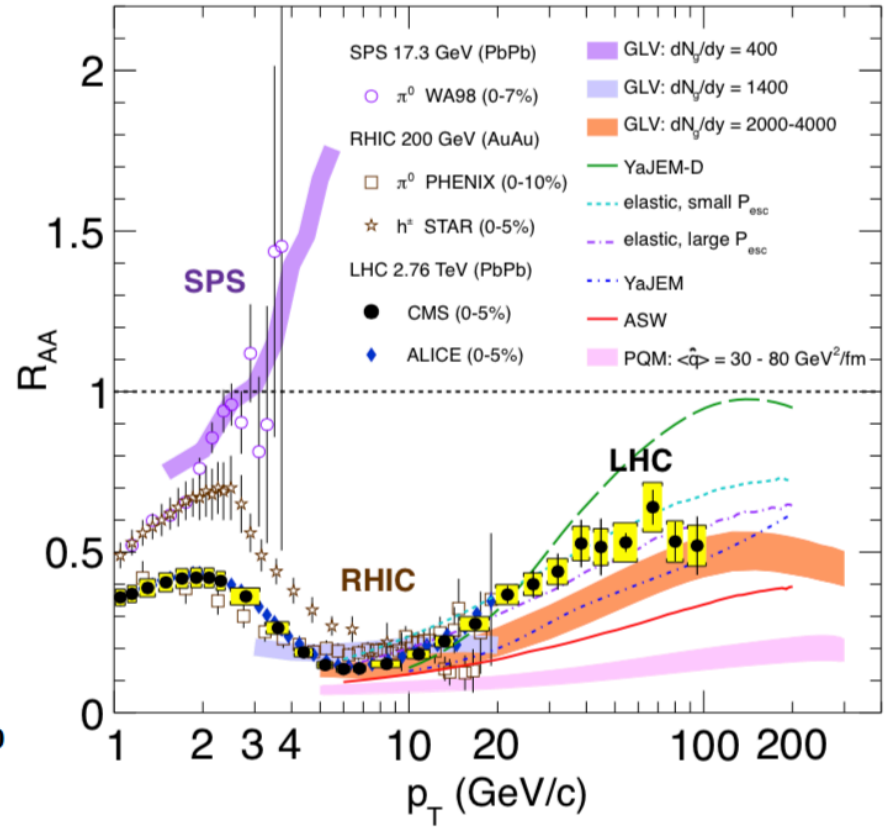

CMS-HIN-10-005

- "Heavy Quark Energy Loss Puzzle"
  - Scattering centers recoil?
  - Realistic path length fluctuations?
- "The surprising transparency of QGP at LHC"
  - The opacity's dependence on density is weaker than linear
  - Smaller coupling at LHC?

The energy loss kernel of fixed coupling CUJET1.0

Radiative: DGLV

$$x_E \frac{dN_g^{n=1}}{dx_E}(\mathbf{x}_0,\phi) = \frac{18 C_R \alpha_s}{\pi^2} \frac{4+n_f}{16+9n_f} \int d\tau\, \rho(\mathbf{z}) \int d^2\mathbf{k} \int d^2\mathbf{q}\, \alpha_s^2 |\tilde{v}(\mathbf{q},\mathbf{z})|^2$$
$$\times \frac{-2(\mathbf{k}-\mathbf{q})}{(\mathbf{k}-\mathbf{q})^2+\chi^2(\mathbf{z})} \left(\frac{\mathbf{k}}{\mathbf{k}^2+\chi^2(\mathbf{z})} - \frac{(\mathbf{k}-\mathbf{q})}{(\mathbf{k}-\mathbf{q})^2+\chi^2(\mathbf{z})} \right)$$
$$\times \left(1 - \cos\left(\frac{(\mathbf{k}-\mathbf{q})^2+\chi^2(\mathbf{z})}{2x_+E}\tau \right) \right)$$
$$\times \left(\frac{x_E}{x_+} \right) J(x_+(x_E))$$

$$|\tilde{v}(\mathbf{q},\mathbf{z})|^2 = \frac{1}{(\mathbf{q}^2+\mu^2(\mathbf{z}))^2}$$

$$\chi^2(\mathbf{z}) = M^2 x_+^2 + m_g^2(\mathbf{z})(1-x_+),\ m_g(\mathbf{z}) = \mu(\mathbf{z})/\sqrt{2}$$

$$\mu^2(\mathbf{z}) = g^2 T(\mathbf{z})^2 (1+n_f/6) = 4\pi\alpha_s T(\mathbf{z})^2 (1+n_f/6)$$

$$x_+(x_E) = \frac{1}{2} x_E \left(1 + \sqrt{1 - \left(\frac{k_\perp}{x_E E} \right)^2} \right) \qquad J(x_+(x_E)) \equiv \frac{dx_+}{dx_E} = \frac{1}{2} \left(1 + \left(1 - \left(\frac{k_\perp}{x_E E} \right)^2 \right)^{-1} \right)$$

Elastic: Thoma-Gyulassy (TG)

$$\frac{dE(\mathbf{z})}{d\tau} = -C_R \pi \alpha_s^2 T(\mathbf{z})^2 \left(1 + \frac{n_f}{6} \right) \log \left(\frac{4T(\mathbf{z})\sqrt{E(\mathbf{z})^2 - M^2}}{\left(E(\mathbf{z}) - \sqrt{E(\mathbf{z})^2 - M^2} + 4T(\mathbf{z}) \right) \mu(\mathbf{z})} \right)$$

CUJET: to solve the heavy quark energy loss puzzle + to explain the surprising transparency of QGP at LHC

❖ Recoiling scattering centers

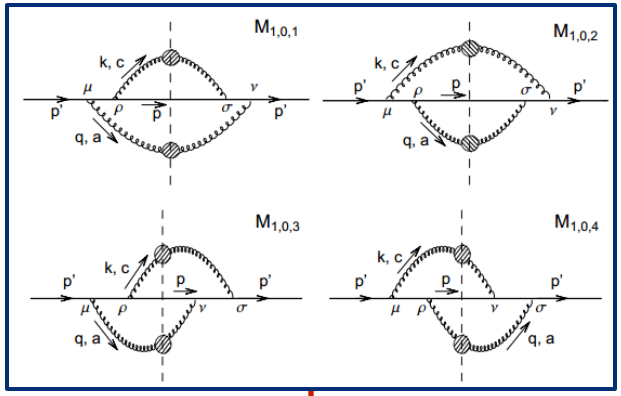

$$\lambda_{\rm dyn} \Longleftrightarrow \lambda_{\rm stat} = \frac{\lambda_{\rm dyn}}{c(n_f)}$$

$$\left[\frac{\mu^2}{\boldsymbol{q}^2(\boldsymbol{q}^2+\mu^2)}\right]_{\rm dyn} \Longleftrightarrow \left[\frac{\mu^2}{(\boldsymbol{q}^2+\mu^2)^2}\right]_{\rm stat}$$

Djordjevic and Heinz, PRC (2008)

❖ Path length fluctuations: $T(\tau_{max}) = T_f$

❖ Multi-scale running strong coupling

$$Q^2 = \mathbf{q}^2$$

$$Q_2^2 = q^2 - M^2 = \frac{\mathbf{k}^2}{x_+(1-x_+)} + \frac{x_+ M^2}{1-x_+} + \frac{m_g^2}{x_+}$$

$$Q^2 = (2T)^2$$

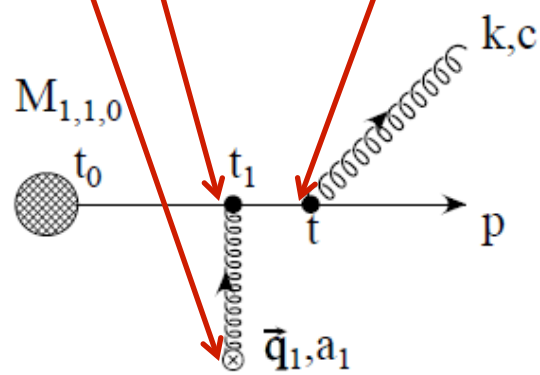

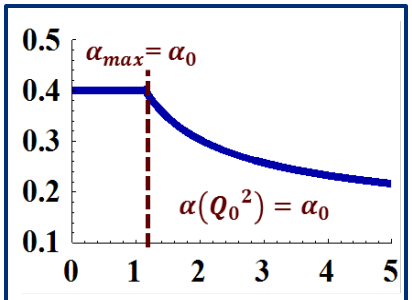

Zakharov, JETP Lett. 2008

Buzzatti, Gyulassy, 2013; JX, Buzzatti, Gyulassy, 2014

❖ Elastic: S. Peigne and A. Peshier, PRD 77, 114017 (2008)

$$\alpha_s^2 \log\frac{4ET}{\mu^2} \longrightarrow \alpha_s(\mu^2)\alpha_s(4ET)\log\frac{4ET}{\mu^2(\alpha_s(4T^2);T)}$$

CUJET2.0: [pQCD+HTL+Elastic] + [2+1D Viscous Hydro]

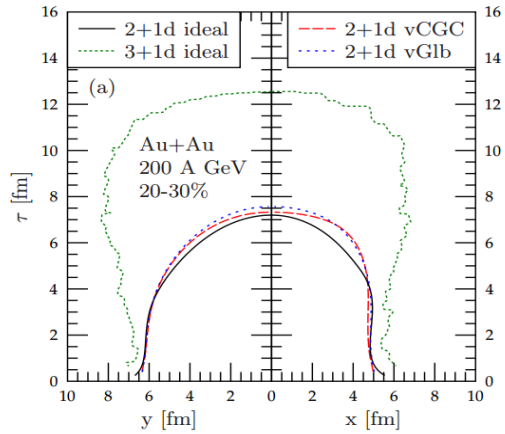

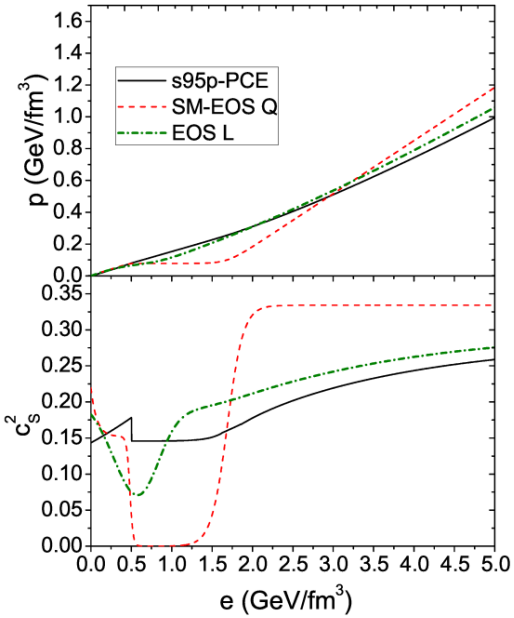

T. Renk, H. Holopainen, U. Heinz and C. Shen, PRC 83, 014910 (2011)
C. Shen, U. Heinz, P. Huovinen and H. Song, PRC 82, 054904 (2010)
H. Song and U. Heinz, PRC 78, 024902 (2008)

- Couple running coupling DGLV opacity series to VISH2+1 transversely expanding QGP fluid fields (T(x,t),v(x,t))

- RHIC Au+Au 200AGeV & LHC Pb+Pb 2.76ATeV
  - Equaiton of State: s95p-v0-PCE
  - Initial Condition: MC-Glauber
  - η/s=0.08
  - Initial Time: 0.6fm/c
  - Cooper-Frye freeze-out temperature: 120MeV

- Viscous hydro backgrounds compatible with measurements of low pT particle production spectra and flow harmonics

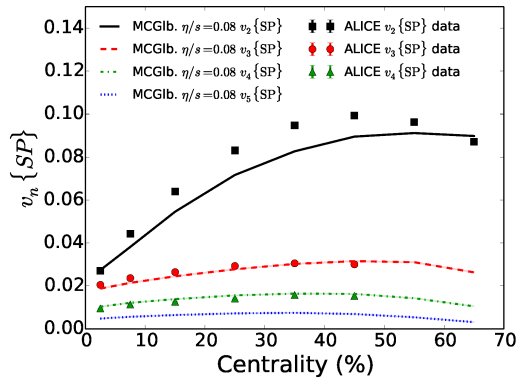

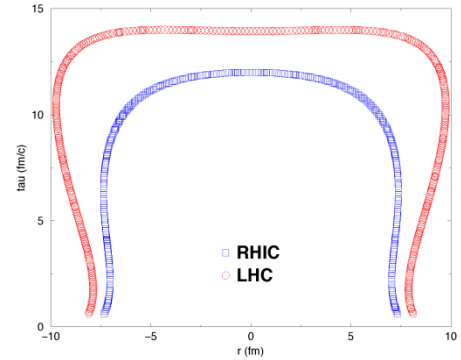

Courtesy of Chun Shen

CUJET2.0: light hadron and open heavy flavor R_{AA}

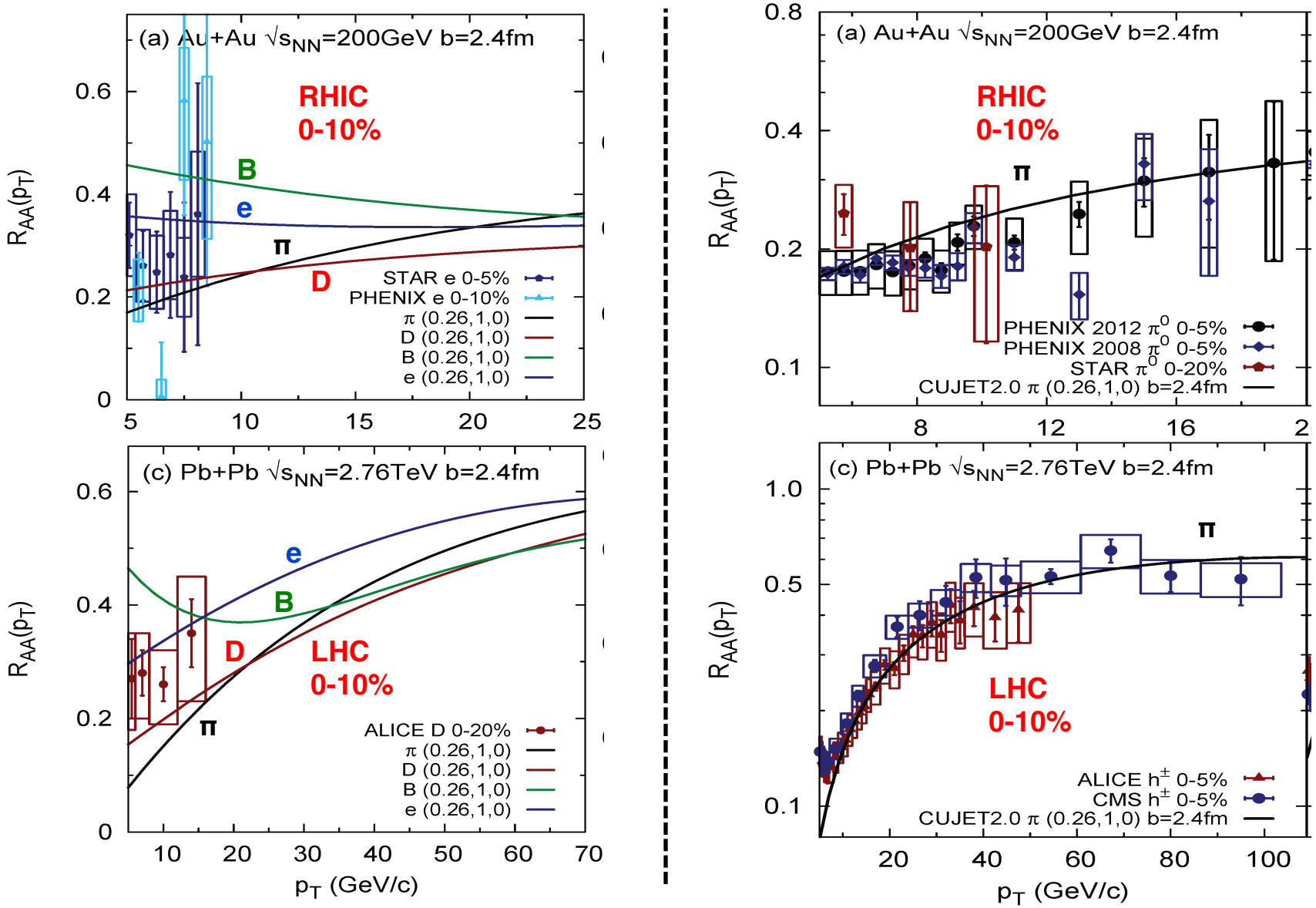

JX, A. Buzzatti, M. Gyulassy, JHEP 1408, 063 (2014)

CUJET2.0: Comparable $R_{AA}(D)$ and $R_{AA}(h)$

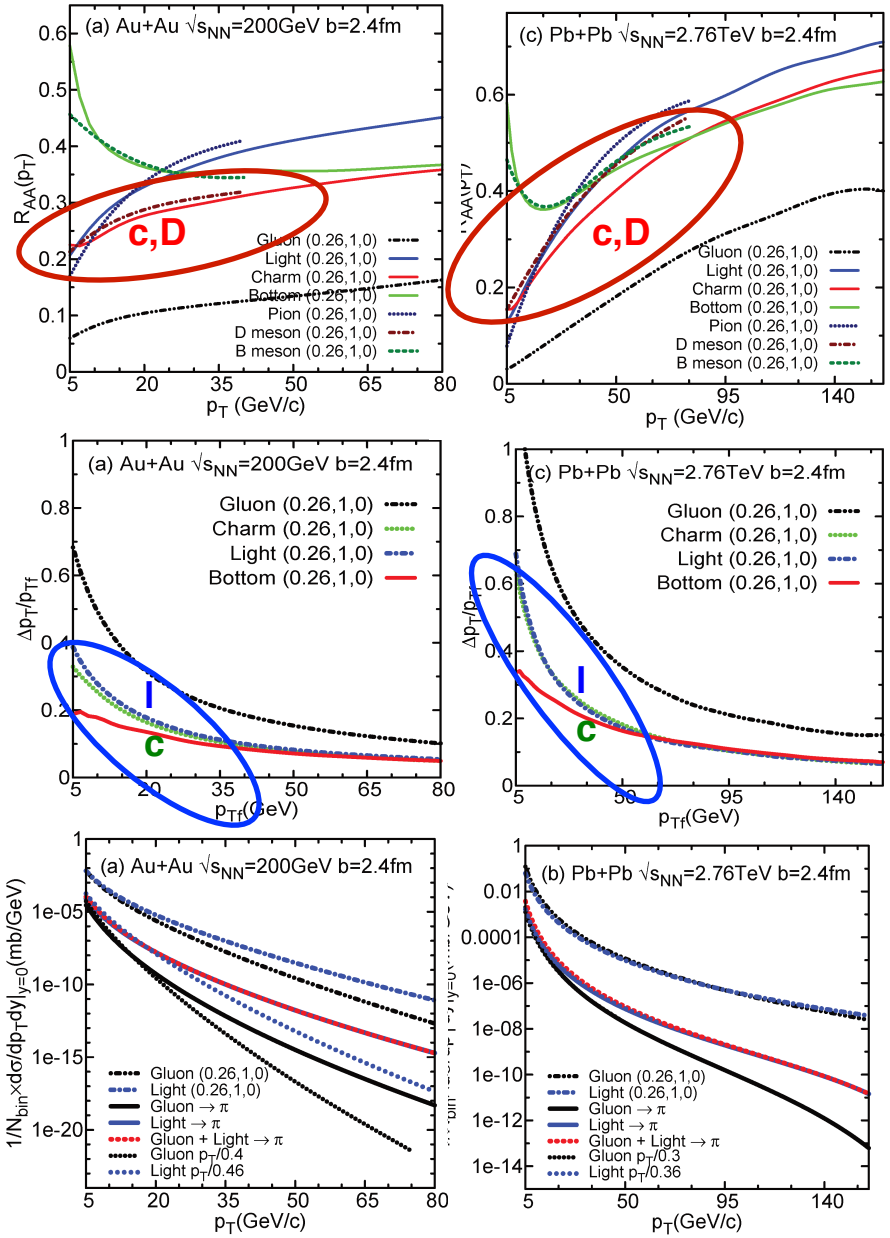

CUJET2.0 @ RHIC **CUJET2.0 @ LHC**

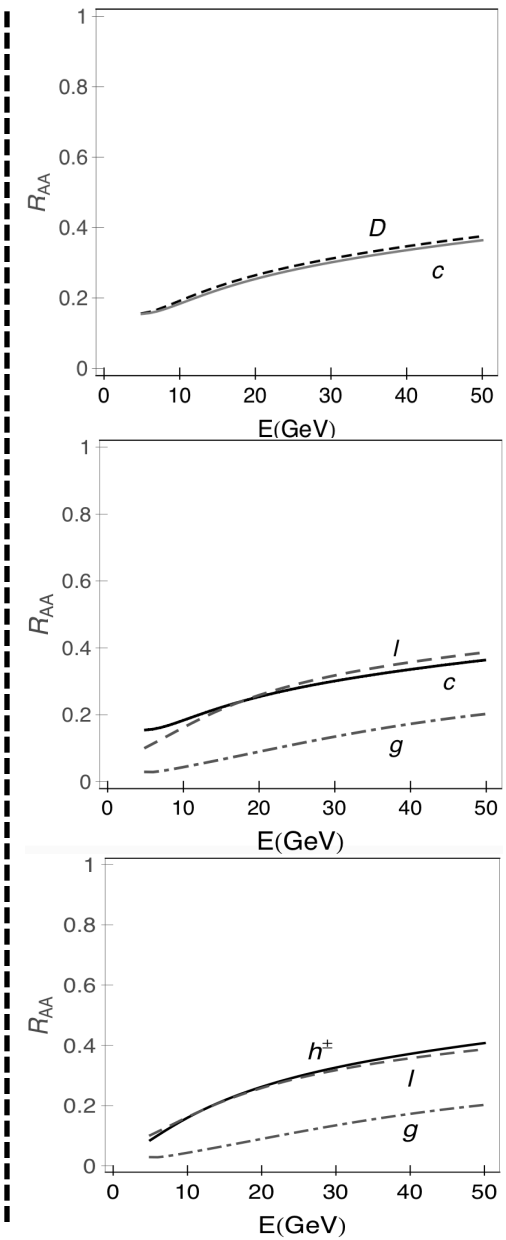

Djordjevic, PRL 2014

- Fragmentation c→D
- $R_{AA}(c) \approx R_{AA}(D)$ [1]

- $\Delta E_g > \Delta E_l \approx \Delta E_c$
  - "≈" comes from interplays between dead cone, LPM and elastic
- $R_{AA}(l) \approx R_{AA}(c)$ [2]

- Distortion from fragmentation
- $R_{AA}(h) \approx R_{AA}(l)$ [3]

[1][2][3]→$R_{AA}(h) \approx R_{AA}(D)$

Jet quenching parameter (qhat) and η/s

$$\hat{q} = \rho \int d^2q_\perp q_\perp^2 \frac{d\sigma}{d^2q_\perp}$$

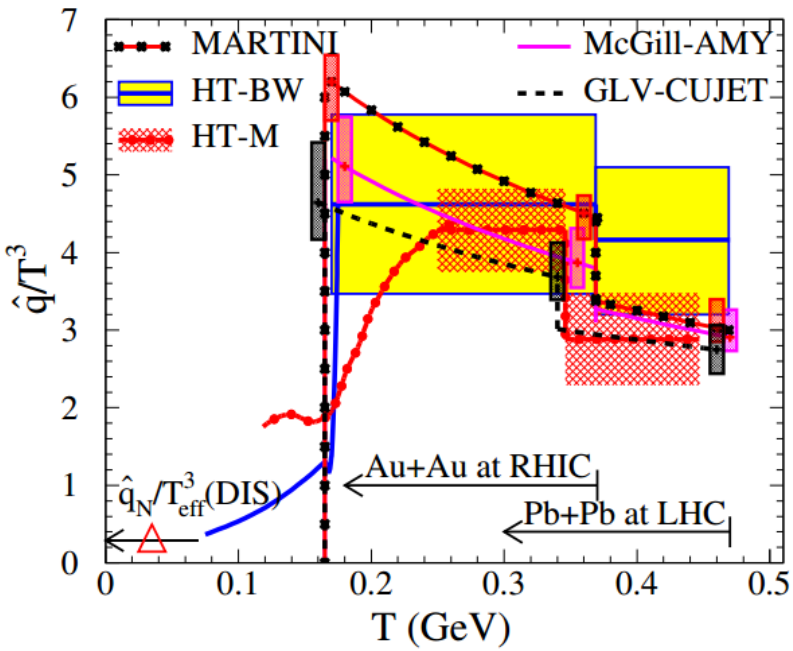

JET Collaboration, PRC 90, 014909 (2014)

$$\frac{\hat{q}}{T^3} \approx \begin{cases} 4.6 \pm 1.2 & \text{at RHIC,} \\ 3.7 \pm 1.4 & \text{at LHC,} \end{cases}$$

$$\hat{q} \approx \begin{cases} 1.2 \pm 0.3 \\ 1.9 \pm 0.7 \end{cases} \text{GeV}^2/\text{fm at} \quad \begin{matrix} T = 370 \text{ MeV,} \\ T = 470 \text{ MeV,} \end{matrix}$$

❖ Kinetic theory estimate of η/s from qhat

$$\eta/s = \frac{1}{s}\frac{4}{15}\sum_a \rho_a \langle p \rangle_a \lambda_a^{tr}$$
$$= \frac{4T}{5s}\sum_a \rho_a \left(\sum_b \rho_b \int_0^{\langle \mathcal{S}_{ab} \rangle/2} dq^2 \frac{4q^2}{\langle \mathcal{S}_{ab} \rangle} \frac{d\sigma_{ab}}{dq^2} \right)^{-1}$$
$$= \frac{18T^3}{5s}\sum_a \rho_a/\hat{q}_a(T, E = 3T) \quad , \qquad (1$$

Danielewicz, Gyulassy, PRD 1985

$$\frac{\eta}{s} \begin{Bmatrix} \approx \\ \gg \end{Bmatrix} 1.25 \frac{T^3}{\hat{q}} \begin{cases} \text{for weak coupling,} \\ \text{for strong coupling.} \end{cases}$$

Majumder, Muller, Wang, PRL 2007

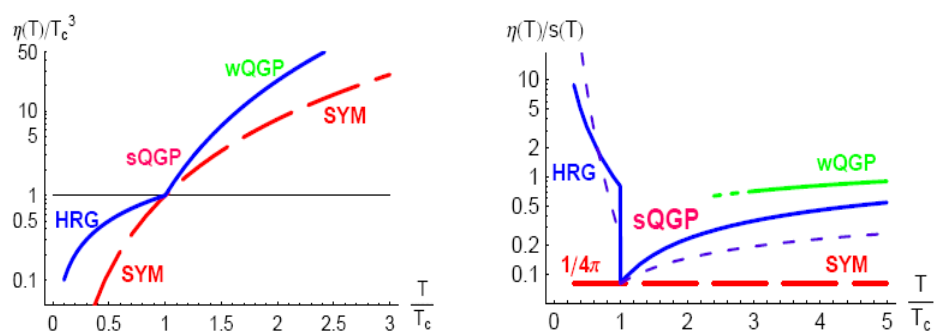

Hirano, Gyulassy, NPA 2006

Jet-medium coupling: from transparency to opaqueness

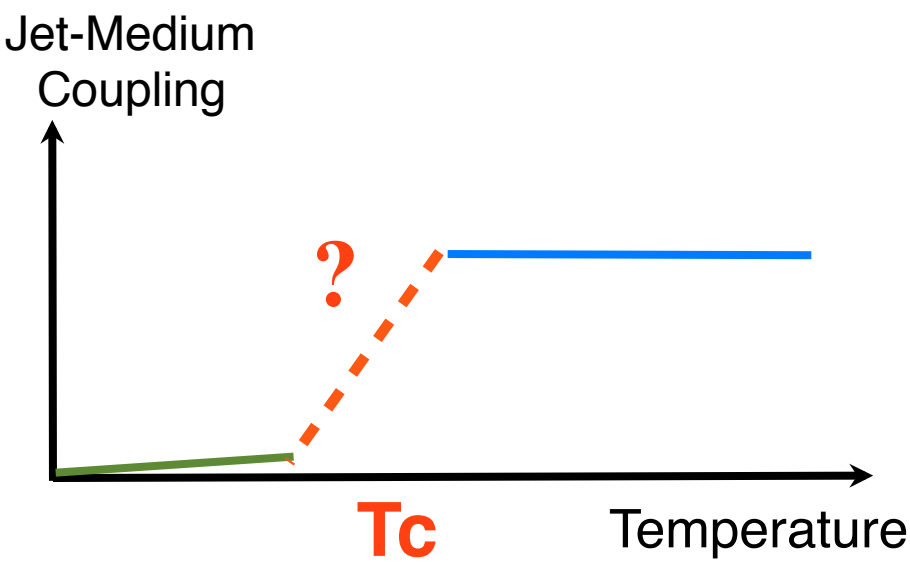

"Waterfall" scenario

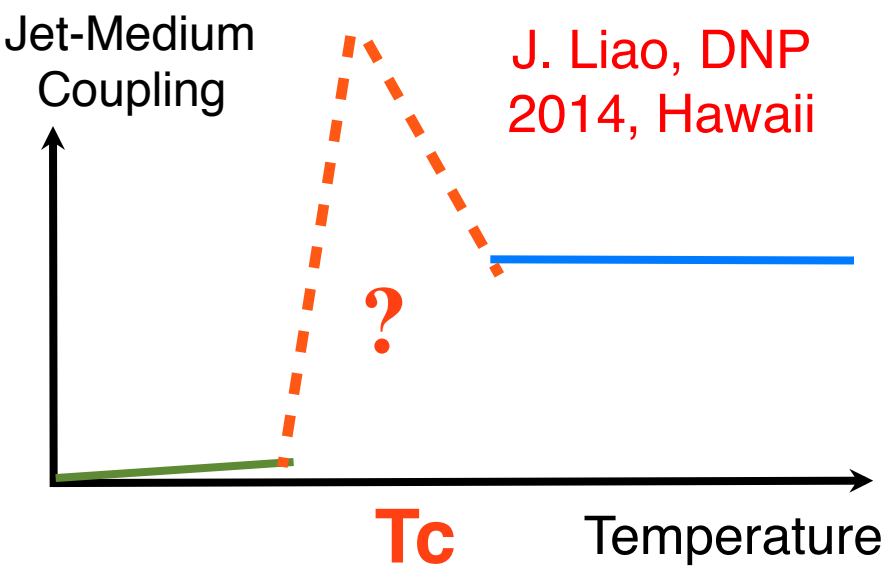

"Volcano" scenario

- How does jet opacity for T>>Tc connect to jet transparency for T<<Tc?
- Is this scenario compatible with the perfect fluidity of QGP near Tc?
- How to systematically implement the microscopic sQGMP model into a jet quenching framework?

CUJET3.0 = pQCD + semi-QGP + mag. monopoles

We now include both color-electric and color-magnetic scattering centers.

Original DGLV has only quark/gluon scattering centers

$$\frac{dE}{dx} \propto \ldots \int_{q^2} \left[\frac{n_e \boxed{(\alpha_s(q^2)\alpha_s(q^2))} f_E^2}{q^2(q^2+f_E^2\mu^2)} + \frac{n_m \boxed{(\alpha_s^e(q^2)\alpha^m(q^2))} f_M^2}{q^2(q^2+f_M^2\mu^2)} \right] \ldots$$

$$\frac{dE}{dx} \propto \ldots \int_{q^2} \frac{n_e\, \alpha_s^2(q^2)\, f_E^2}{q^2(q^2+f_E^2\mu^2)} \ldots$$

$$\frac{dE}{dx} \propto \ldots \int_{q^2} \frac{n_T}{(q^2+f_E^2\mu^2)(q^2+f_M^2\mu^2)} \times \kappa(q^2,T)$$

$$\kappa(q^2,T) \equiv \boxed{\alpha_s^2(q^2)}\, \chi_T \left(f_E^2 + \frac{f_E^2 f_M^2 \mu^2}{q^2}\right) + (1-\chi_T)\left(f_M^2 + \frac{f_E^2 f_M^2 \mu^2}{q^2}\right)$$

=1, by Dirac Quantization

$$\chi_T = c_q L + c_g L^2$$

Polyakov Loop suppressed color electric component

$$f_E = \sqrt{\chi_T}$$

$$f_M = C_m g_T$$

$$L(\mathbf{x}) = \frac{1}{N_c} \mathrm{tr}\mathcal{P} \exp\left[ig \int_0^{1/T} A_4(\tau,\mathbf{x}) d\tau\right]$$

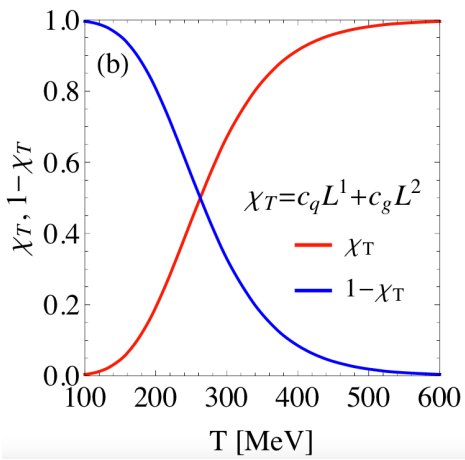

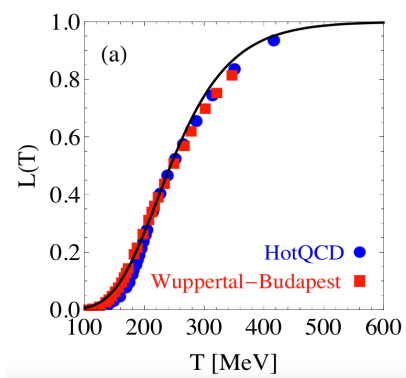

Bazavov et al., PRD 80 (2009)
Borsanyi et al., JHEP 09 (2010)

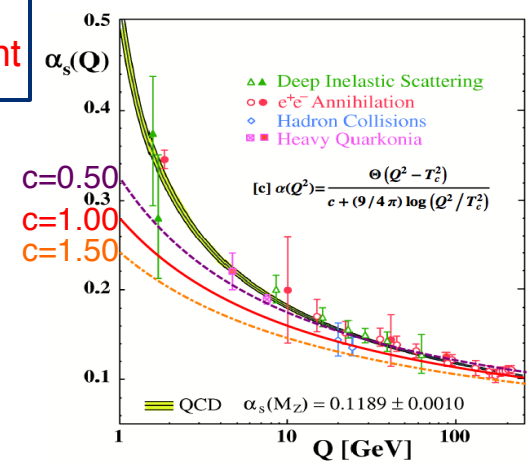

$$\alpha_s^2(q^2) \approx [1/[c + (9/2\pi) Log(q/\Lambda)]]^2$$

Lattice Constraints: Polyakov Loop, EOS, Screening Masses

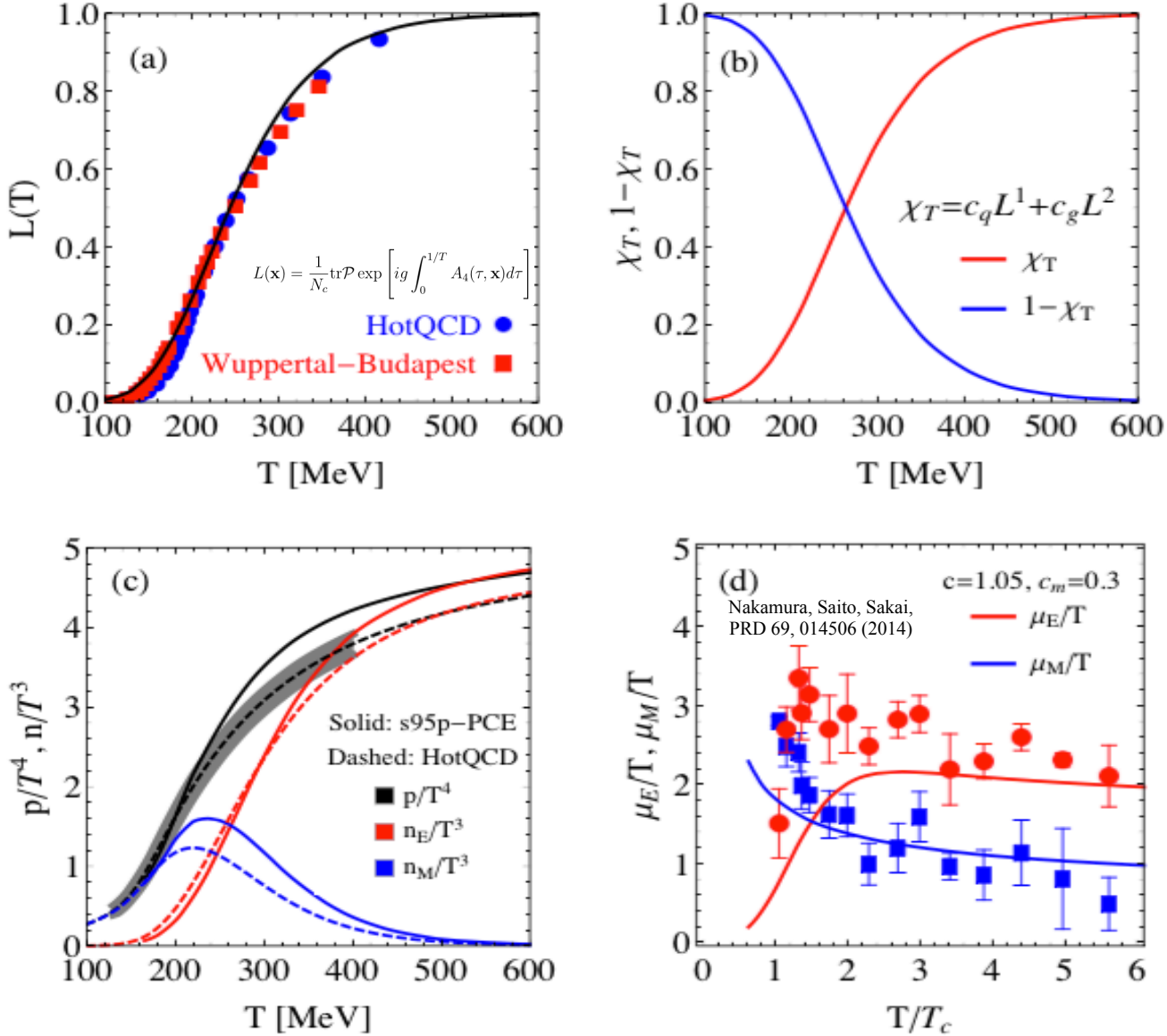

❖ The CUJET3.0 implementations of electric and magnetic components are well constrained by available lattice data. The only adjustable parameter in this model is “c”.

CUJET3.0 simultaneously describes high pT (R_{AA}+v_2)*(light+heavy)*(RHIC+LHC)

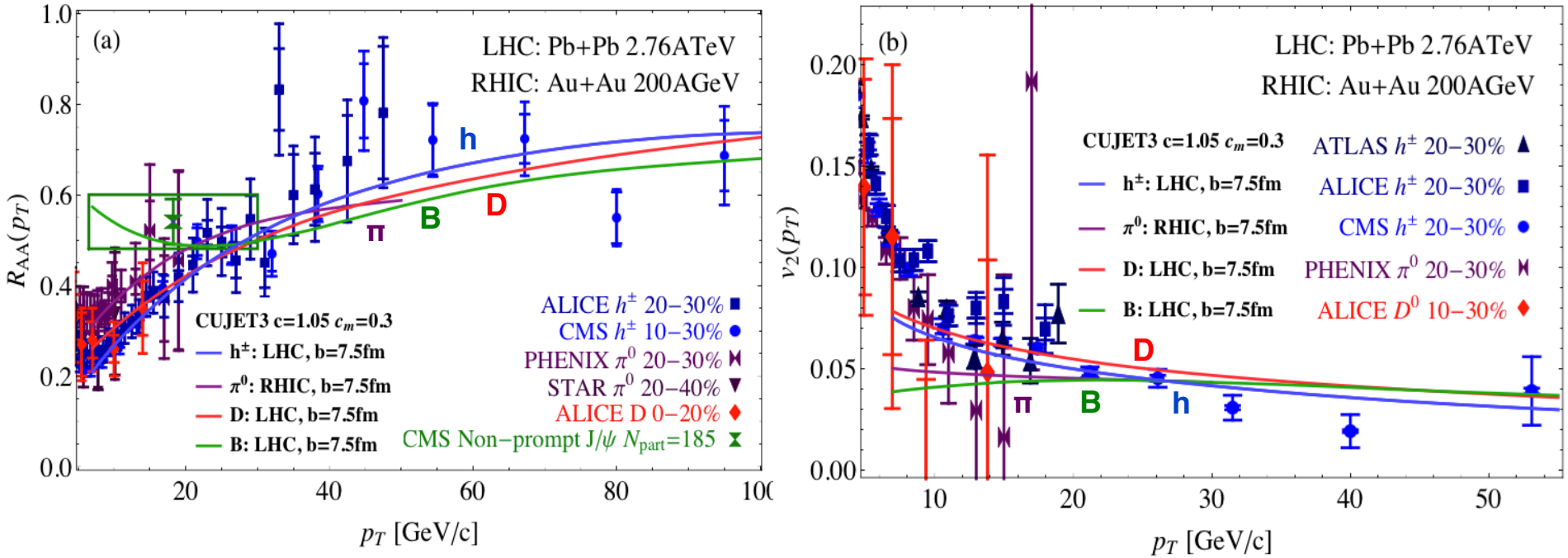

JX, J. Liao, M. Gyulassy, arXiv:1411.3673

The combined set of observables

(R_{AA}+V_2)*(RHIC+LHC)*(pion+D+B)

are consistently accounted for (within present experimental errors) in the CUJET3.0 framework using lattice data constrained sQGMP near Tc + pQCD jet quenching

Open charm's and beauty's high p_T R_{AA} and v_2 at RHIC and LHC (20-30% centrality) from CUJET3.0

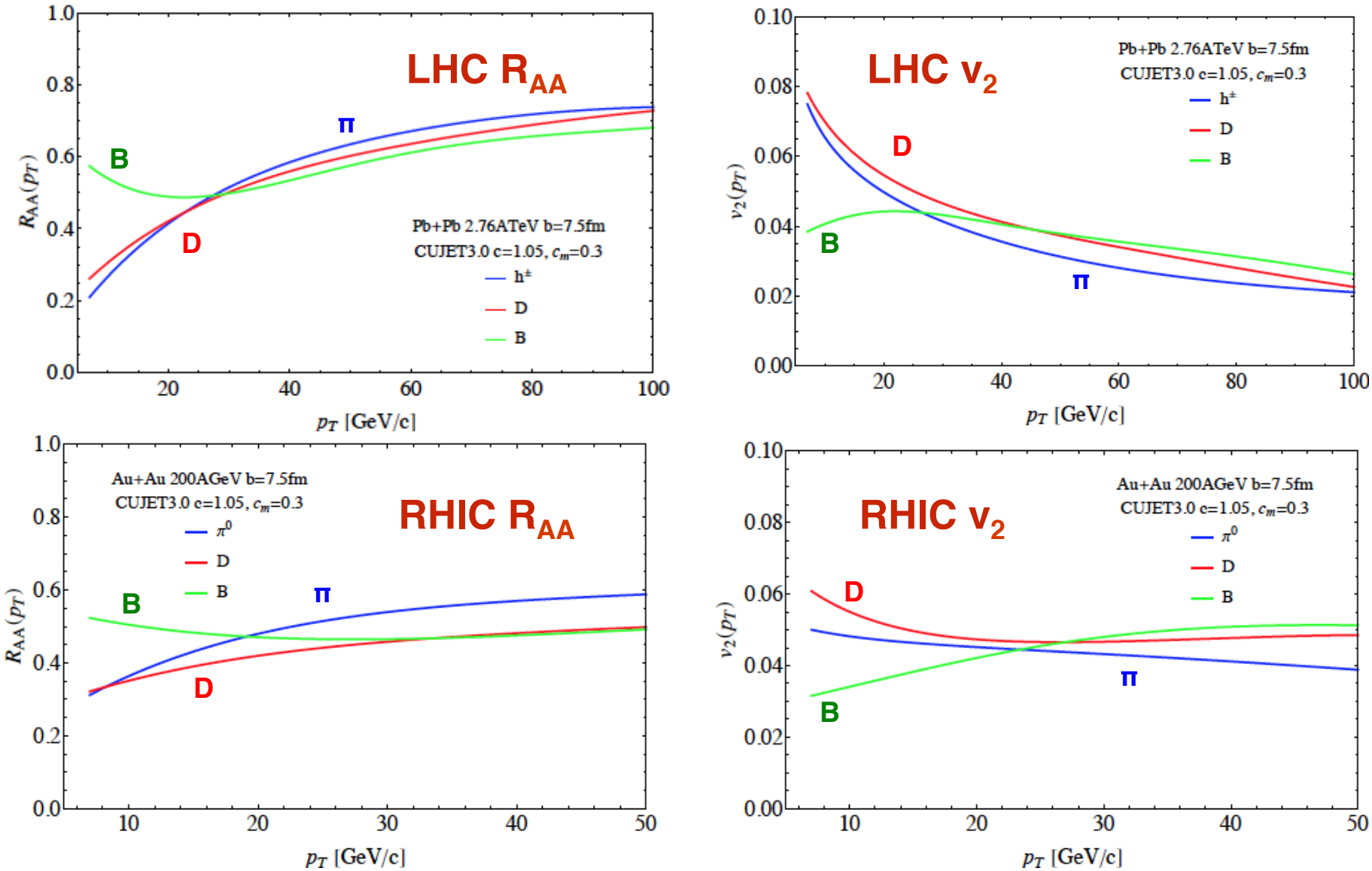

CUJET3.0: HF Decay Electron RAA & v2

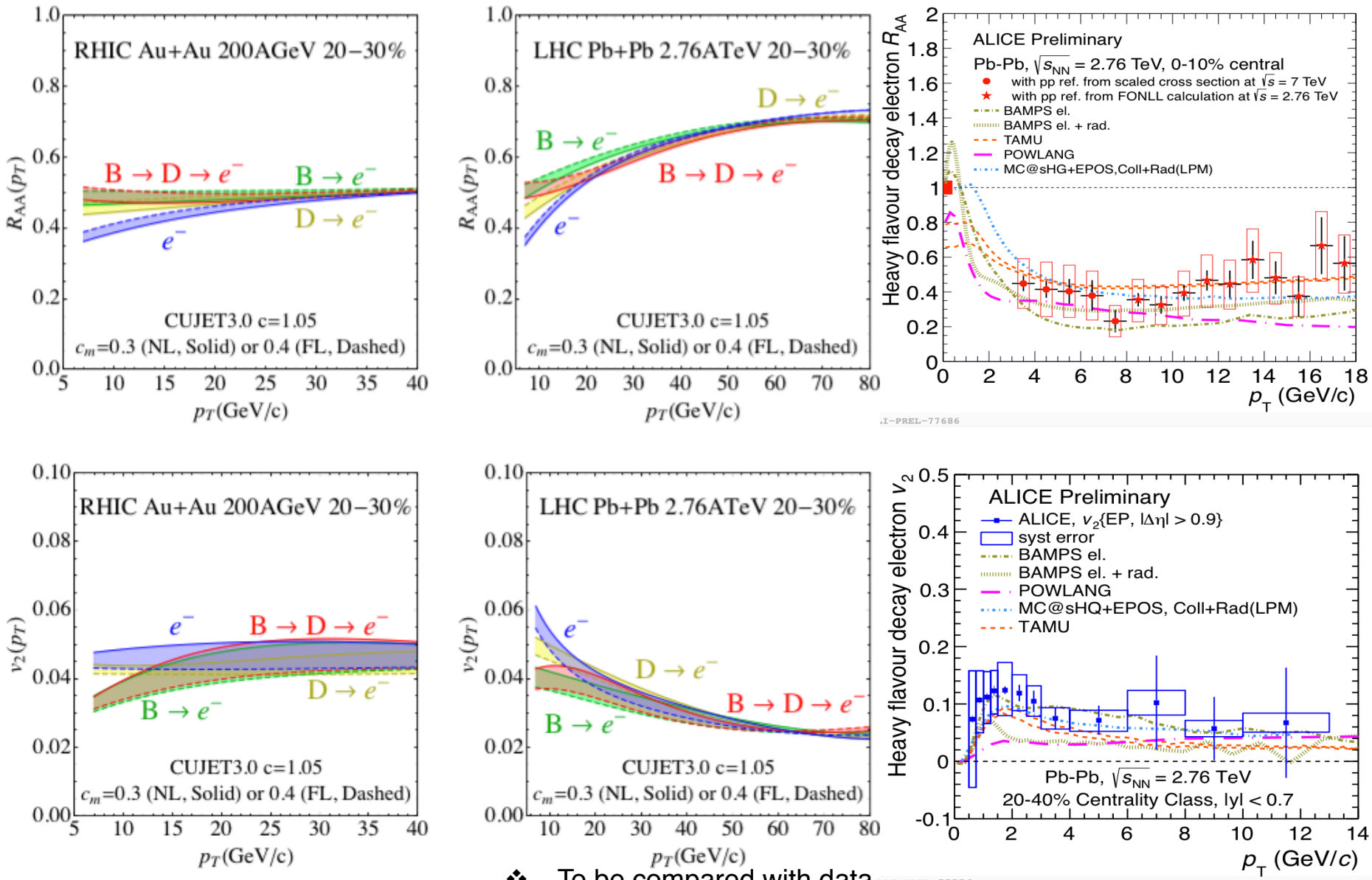

- To be compared with data

CUJET3.0: qhat(E,T) for quark jets in sQGMP

Liu et al. PRL 2006

$\hat{q} \approx 26.69\sqrt{\lambda/4\pi}T^3$

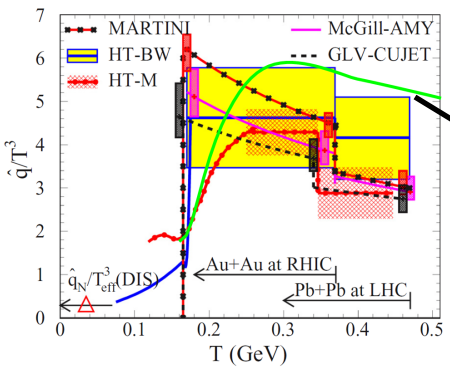

JET Collaboration, PRC 2014

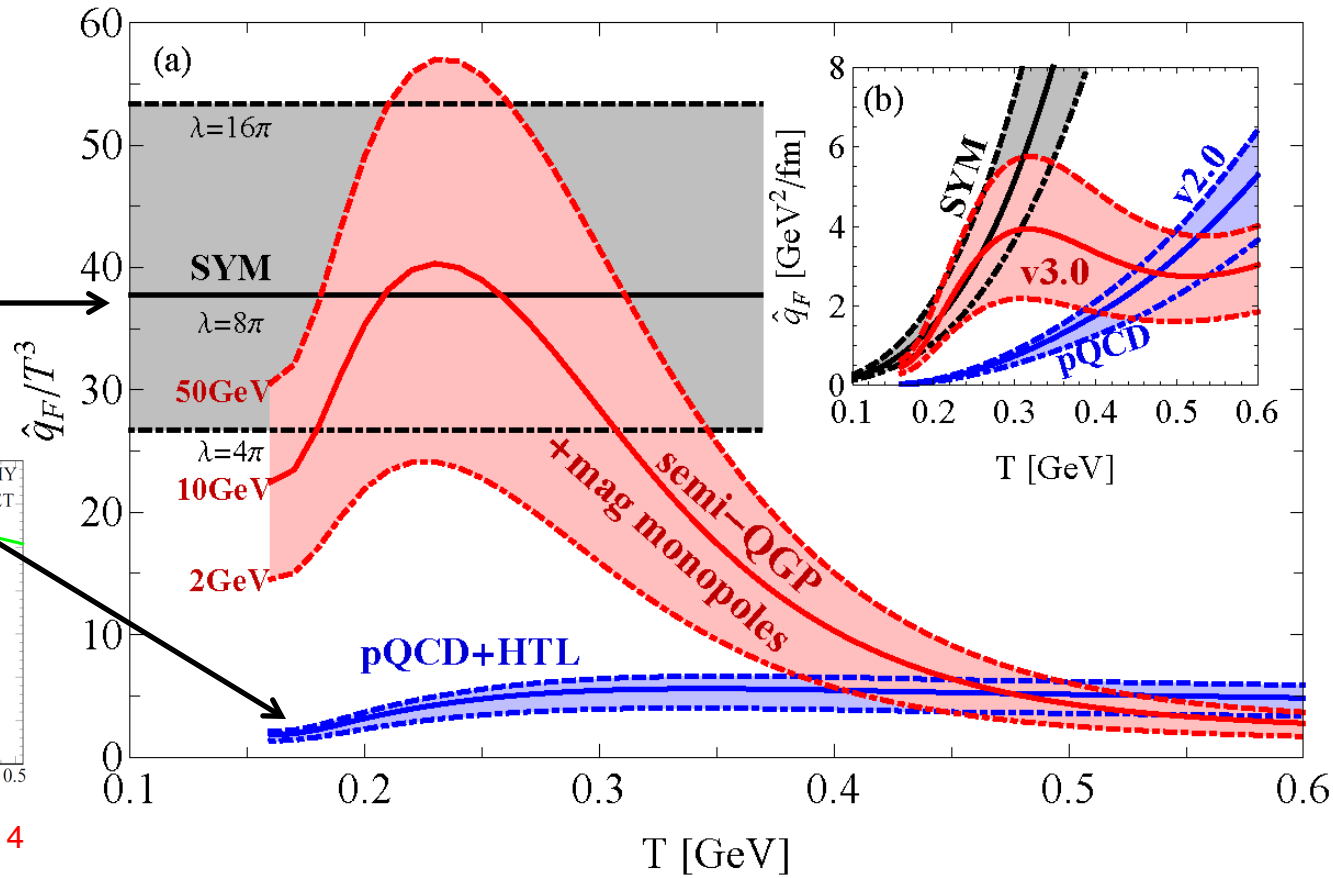

$$\hat{q}_F = \int_0^{6ET} dq^2 \frac{2\pi q^2}{(q^2+f_E^2\mu^2)(q^2+f_M^2\mu^2)}\rho(T) \times \left[(C_{qq}f_q + C_{qg}f_g)\alpha_s^2(q^2) + C_{qm}(1-f_q-f_g)\right]$$

$$f_q = c_q L(T),\ f_g = c_g L(T)^2$$

$$\rho(T) \sim p(T)/T$$

p(T) from s95p-PCE EOS

- CUJET3.0 solution exhibits a “volcano” interpolation of qhat/T^3 between strong “AdS-like” sQGP at T=200-350MeV to more transparent “HTL-like” QGP for T>400MeV

pQCD jet quenching + sQGMP: η/s(T)

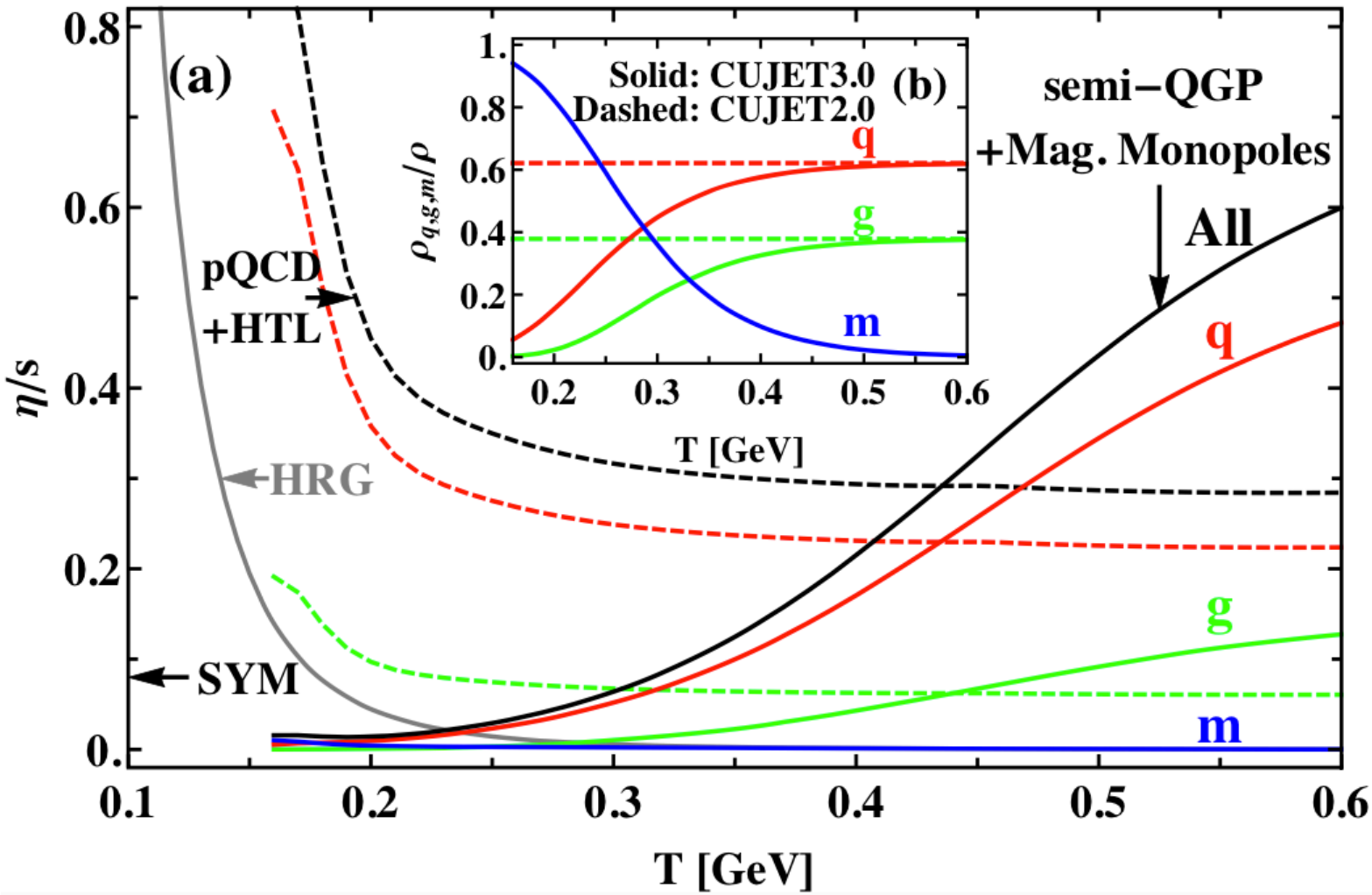

- CUJET3.0 provides a quantitative connection between the jet transport properties controlling the hard jet quenching observables and the bulk viscous transport properties controlling the soft "perfect fluidity" of QGP observed at RHIC and LHC.

Near-Tc properties of sQGMP are special!

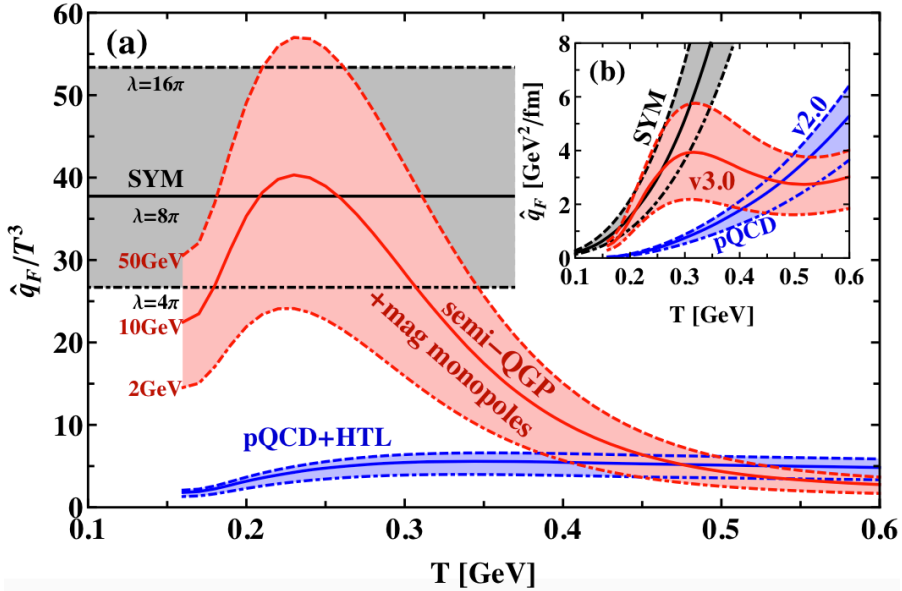

Jet transport coefficient qhat/T^3 computed from CUJET3.0 shows a prominent peak near Tc!

Shear viscosity, η/s, computed from CUJET3.0 shows a clear minimum near Tc and a rapid rise at high T!

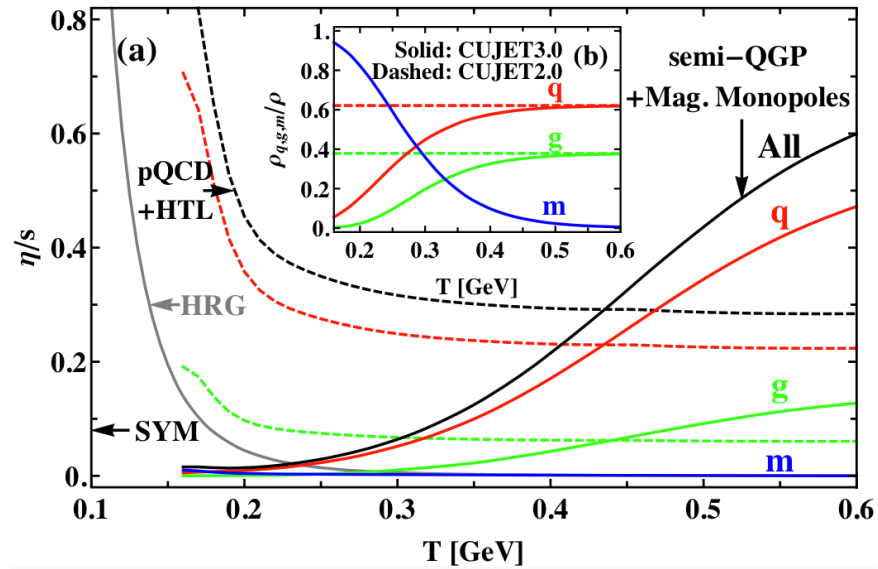

CUJET3.0 = [pQCD] + [semi-QGP] + [magnetic monopoles] bridges the "soft" bulk perfect fluidity and the "hard" jet quenching (η/s~T^3/qhat)

BES@RHIC and LHC are both essential to constrain and map out the strongly non-conformal QCD confinement transition physics

Summary

- CUJET2.0 = [rcDGLV+Elastic] + [2+1D Viscous Hydro] solves the "heavy quark energy loss puzzle" and explains the "surprising transparency of QGP at LHC"

- Combining the pQCD jet quenching kernal and the microscopic semi-Quark-Gluon Monopole Plasma (sQGMP) model, CUJET3.0 describes (R_{AA}+v_2) × (pion+D+B) × (RHIC+LHC) simultaneously
  - qhat from CUJET3.0 smoothly bridges the N=4 SYM limit near Tc and the HTL pQCD limit at high T
  - eta/s from CUJET3.0 approaches the perfect fluidity ~0.1 near Tc, and rises rapidly at high T

Thank you!

Backup

Bulk & jet transport properties

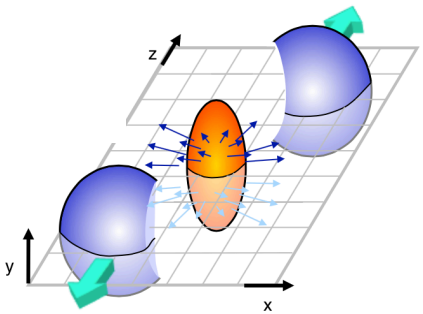

Bulk: nonperturbative

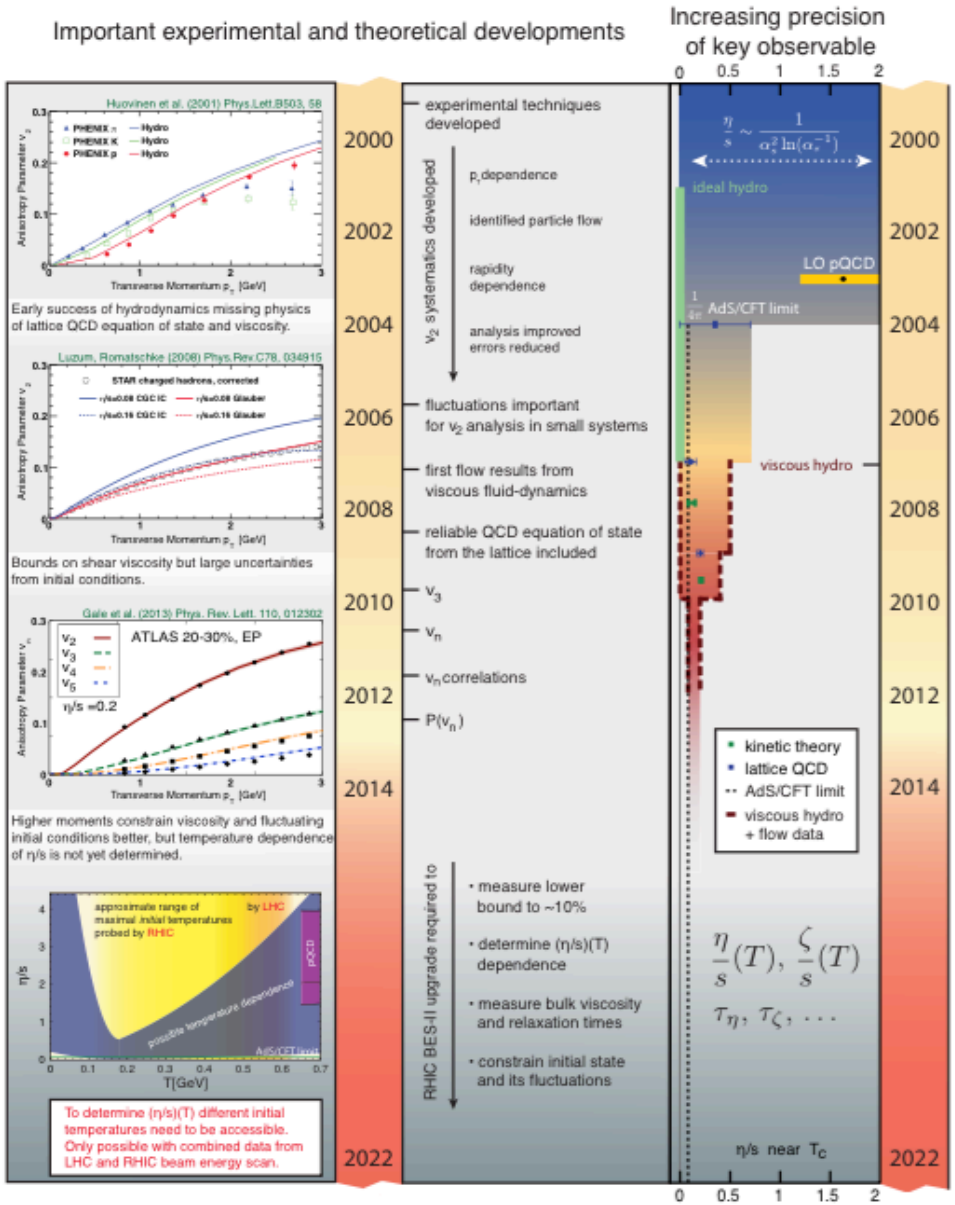

Gale, Jeon, Schenke, 2013

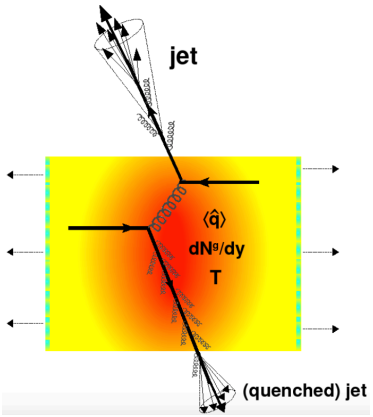

Jet quenching: perturbative

More on the strong suppression of HF decay lepton at intermediate and high pT

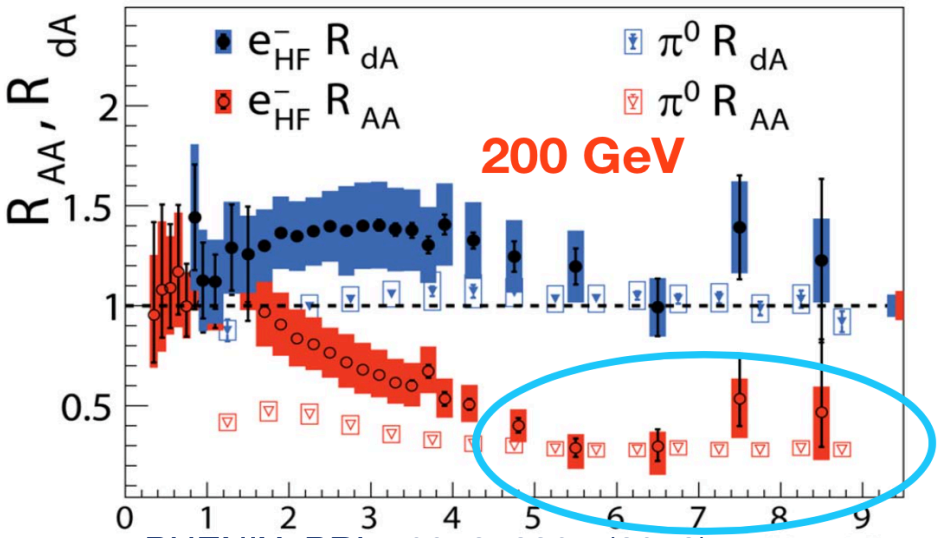

PHENIX, PRL 109, 242301 (2012)

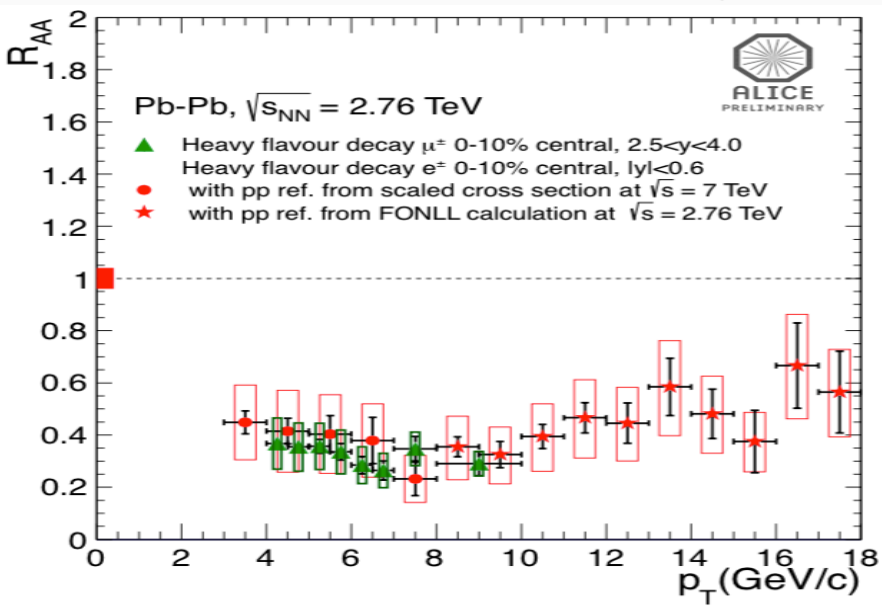

- The suppression is a final state effect due to in-medium parton energy loss
- $R_{AA}(c \rightarrow e) \approx R_{AA}(\pi)$
- $R_{AA}(c,b \rightarrow e)$ is overpredicted at RHIC
  - Heavy quark energy loss puzzle

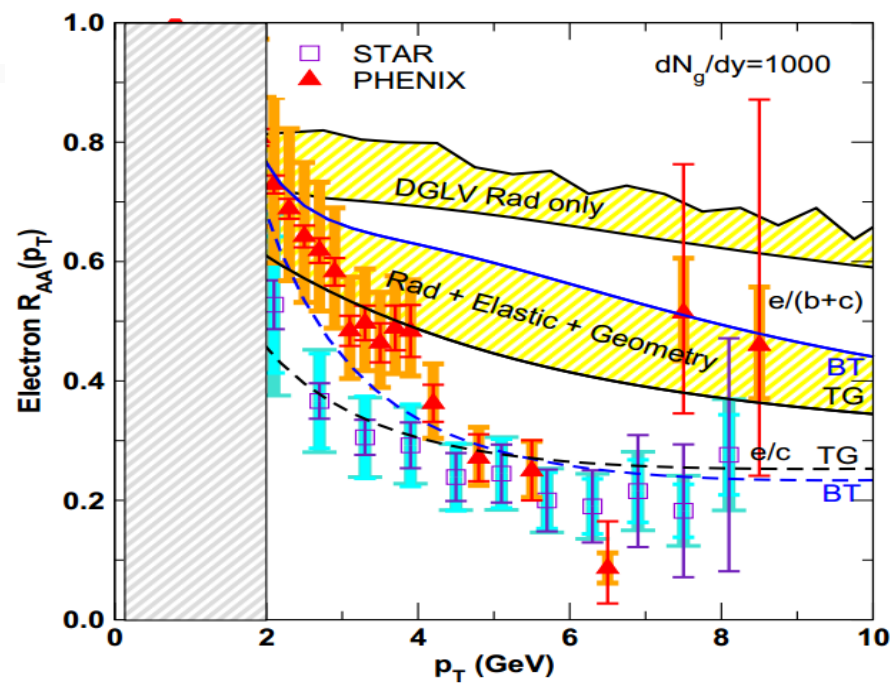

WHDG, NPA 784, 426 (2007)

Comparable D mesons and charged particles R_{AA}

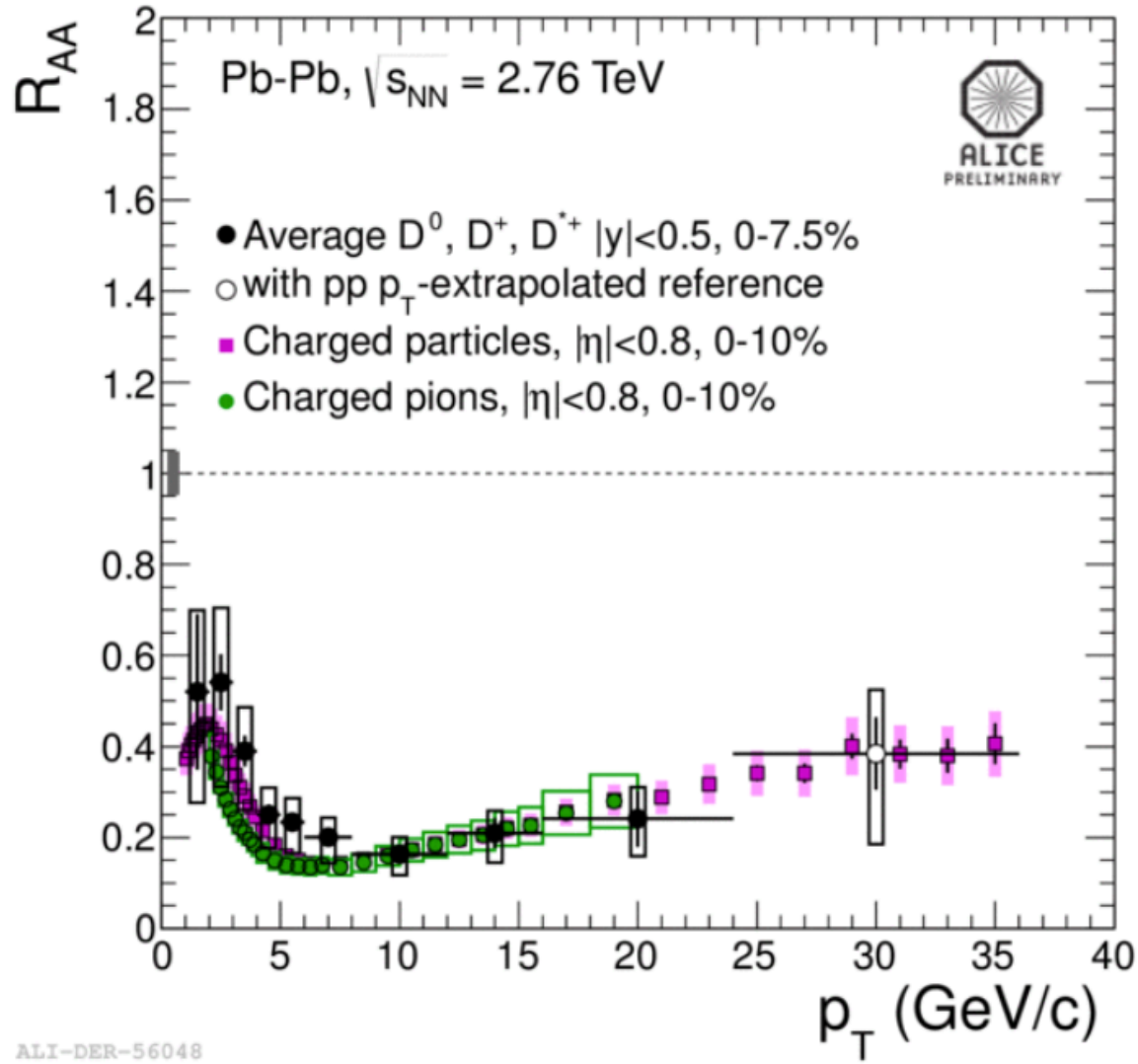

- Comparable results for D and π suppressions within uncertainties
- Consistency of the color charge and mass dependence $\Delta E_g > \Delta E_{u,d,s} > \Delta E_c > \Delta E_b$?

More about the multi-scale running coupling

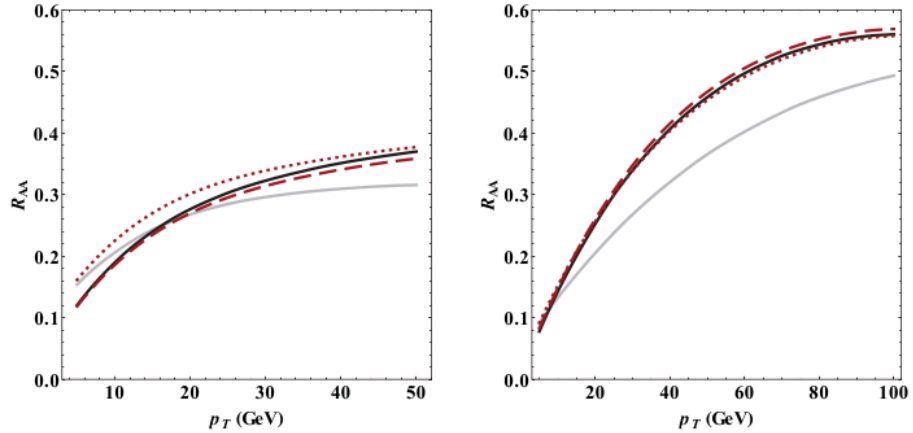

Figure 1. Fixed and running coupling pion R_{AA} results are compared side to side at RHIC (*left*) and LHC (*right*) in CUJET with Glauber static transverse plus Bjorken longitudinal expanding background. The gray opaque curves use a fixed coupling with $\alpha_s = 0.3$, while the black curves use a running coupling with $\alpha_{\max} = 0.4$. The difference is notable, especially in the higher energy range available at the LHC, while RHIC results are left almost unchanged. The sensitivity to the variation of running scales Q_i (cf. eq. (2.1) and following) is measured by the red curves: on one side we decrease the value of all scales Q_i by 50% and lower $\alpha_{\max}$ to 0.3 (red dashed), on the other we increase all scales Q_i by 25% and increase at the same time $\alpha_{\max}$ to 0.6 (red dotted). $\alpha_{\max}$ is constrained to fit $R_{AA}^{\pi,LHC}(p_T \approx 30\,\text{GeV}) = 0.35$.

- Which running scale dominates?

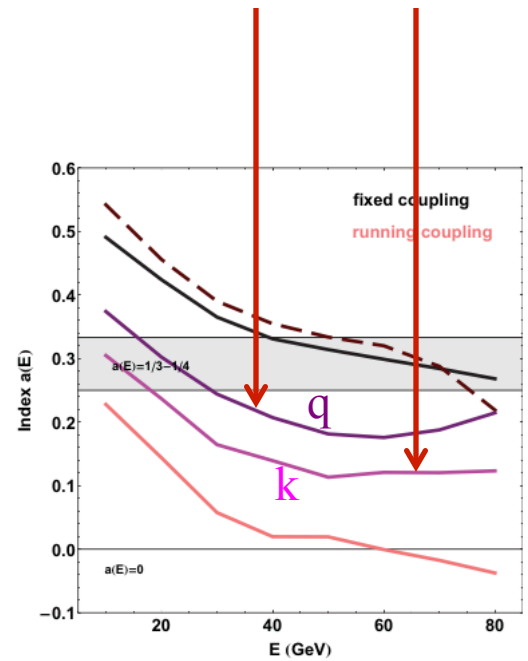

Figure 2. Energy loss index $a(E)$ (cf. eq. (2.9)) for different assumptions of the running coupling in CUJET: fixed effective $\alpha_s = 0.3$ (black), only thermal coupling running (dashed red), only $\alpha_s^2(\mathbf{q}^2)$ running (purple), only $\alpha_s^2(\mathbf{k}^2/(x(1-x)))$ running (magenta), all couplings running (pink). The saturated $\alpha_{\max}$ value is chosen to be equal to 0.4, which corresponds to approximately $Q_0 \sim 1\,\text{GeV}$. The plot shows the energy loss of a light quark ($M = 0.2\,\text{GeV}$) traveling from the origin of the transverse plane and through a gluonic plasma ($n_f = 0$) of size $L = 5\,\text{fm}$, whose density profile is generated from Glauber model and resembles the medium created in a Pb+Pb $\sqrt{s_{NN}} = 2.76\,\text{TeV}$ $b = 0\,\text{fm}$ collision.

- Uncertainties in running scales

Heavy Quark Puzzle: Dead Cone

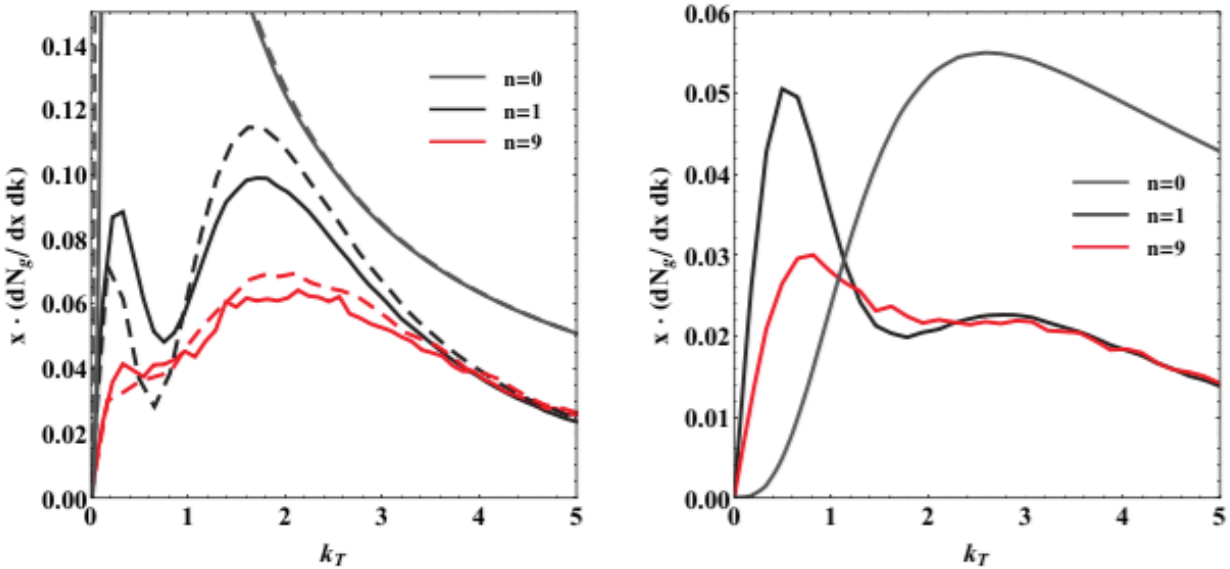

Figure 18. Radiation spectrum for charm (*left*) and bottom (*right*) quarks traversing a brick of thickness $L = 5\,\text{fm}$, with $E = 20\,\text{GeV}$ and $\omega = 5\,\text{GeV}$ ($x = 0.25$). The masses are assumed $M_c = 1.2\,\text{GeV}$ and $M_b = 4.75\,\text{GeV}$. The dashed curves represent the spectrum of a light jet of mass $M_l = 0.2\,\text{GeV}$. Notice the similarity between the light and charm spectra, as opposed to the bottom one. The vacuum spectrum radiation is added to the plot (gray curve), showing the radiation dead cone for respective quark jets. Other parameters used in the calculation are: $\lambda = 1.16\,\text{fm}$, $\mu = 0.5\,\text{GeV}$, $m_g = 0.356\,\text{GeV}$, $T = 0.258\,\text{GeV}$, $n_f = 0$, $\alpha_s = 0.3$.

$$x\frac{dN_g^0}{dxd\mathbf{k}} \sim \frac{\mathbf{k}^2}{(\mathbf{k}^2+\chi^2)^2}$$

$$\theta < \chi/\omega = \sqrt{M^2x^2 + m_g^2(1-x)}/(xE)$$

JX, Buzzatti, Gyulassy, JHEP 1408, 063 (2014)

Heavy quark puzzle: Where are the problems?

- Jet path length
- pp spectra
- Scattering centers recoil

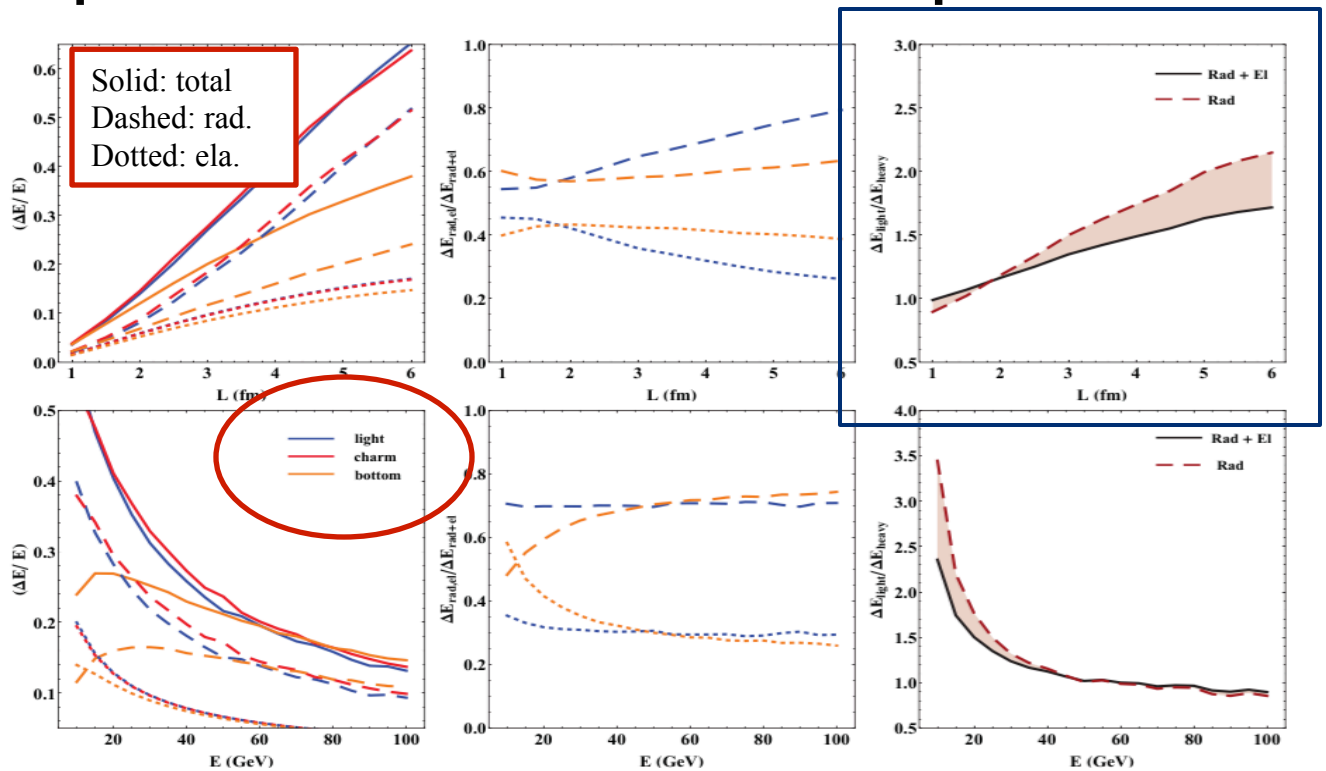

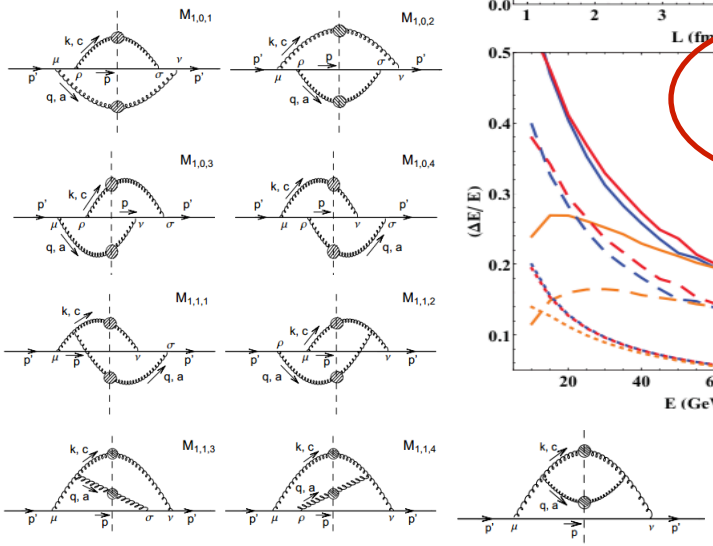

$$\lambda_{\rm dyn} \Longleftrightarrow \lambda_{\rm stat} = \frac{\lambda_{\rm dyn}}{c(n_f)}$$

$$\left[\frac{\mu^2}{\boldsymbol{q}^2(\boldsymbol{q}^2+\mu^2)}\right]_{\rm dyn} \Longleftrightarrow \left[\frac{\mu^2}{(\boldsymbol{q}^2+\mu^2)^2}\right]_{\rm stat}$$

Djordjevic and Heinz, PRC (2008)

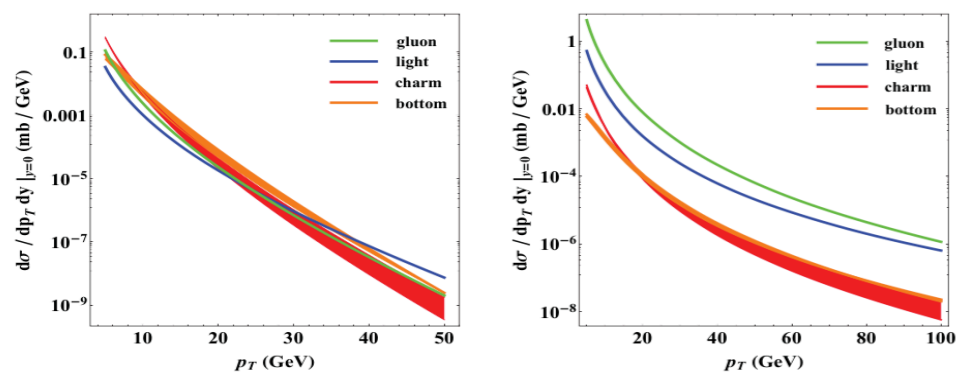

Figure 24. pQCD p+p production spectra at $\sqrt{s_{NN}} = 200\,\text{GeV}$ (RHIC, *left*) and $\sqrt{s_{NN}} = 2.76\,\text{TeV}$ (LHC, *right*). Notice how steeper the RHIC spectra are compared to LHC ones. The light

CUJET: Answer to – Intersection of R_{AA}(B) and R_{AA}(D/π/h)

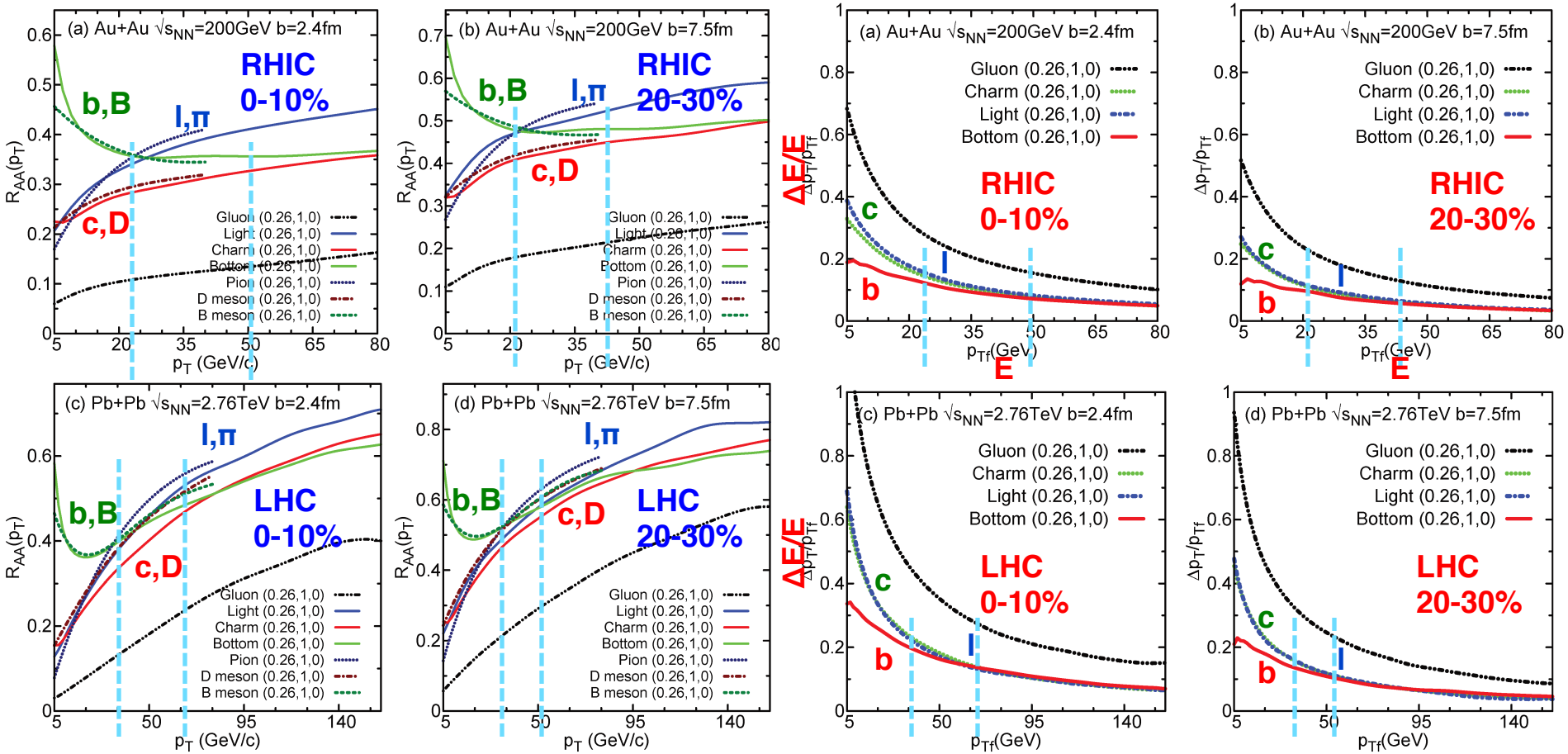

$$\frac{d\bar{\sigma}^{AA\to h}}{d^3p_f} \equiv \frac{1}{N_{bin}}\frac{d\sigma^{AA\to h}}{d^3p_f} = \frac{d\sigma^{pp\to q}}{d^3p_i} \otimes P(E_i(p_i)\to E_f(p_f)) \otimes D(q\to h)$$

- The shape of pp baseline and mechanism of energy loss combined to induce the intersection
- B & D: mechanism of energy loss; B & π/h: shape of pp baseline
- Centrality ↗ Intersection p_T ↘ (B&D's intersecting p_T shifted more than B&π/h's)

CUJET2.0: high pT v2 with reaction plane dependent jet-medium coupling

- As less as a 10% increase of the path averaged coupling strength from in- to out-of-reaction plane can generate a simultaneous description of light hadron's RAA and v2 at both RHIC and LHC

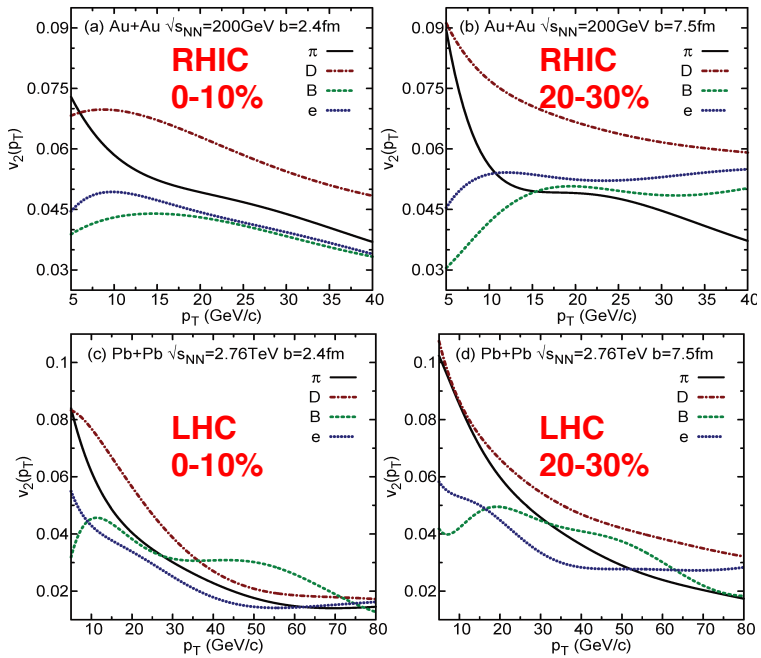

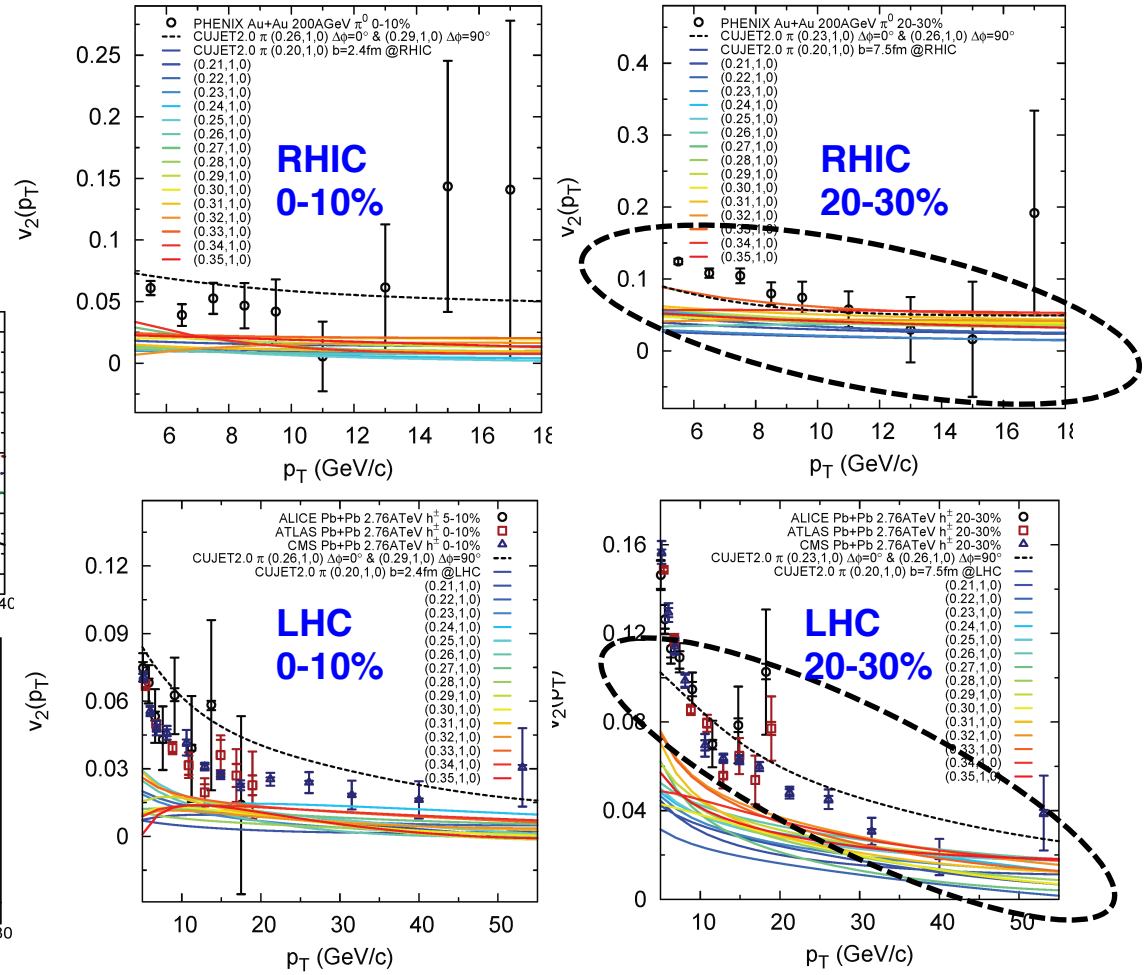

JX, Buzzatti, Gyualssy, JHEP 1408, 063 (2014)

- The high pT v2 is very sensitive to the jet-medium coupling's local temperature dependence

More on the Polyakov Loop

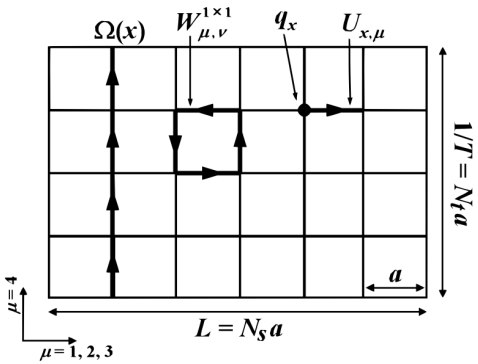

$$U_{x,\mu} = \mathcal{P}\exp\left[ig\int_x^{x+\hat{\mu}} dx_\mu A_\mu(x)\right]$$

$$W^{1\times1}_{\mu\nu}(x) \equiv U_{x,\mu}U_{x+\hat{\mu},\nu}U^\dagger_{x+\hat{\nu},\mu}U^\dagger_{x,\nu}.$$

$$L(\mathbf{x}) = \frac{1}{N_c}\mathrm{tr}\mathcal{P}\exp\left[ig\int_0^{1/T} A_4(\tau,\mathbf{x})d\tau\right] \equiv \frac{1}{N_c}\mathrm{tr}\Omega(\mathbf{x})$$

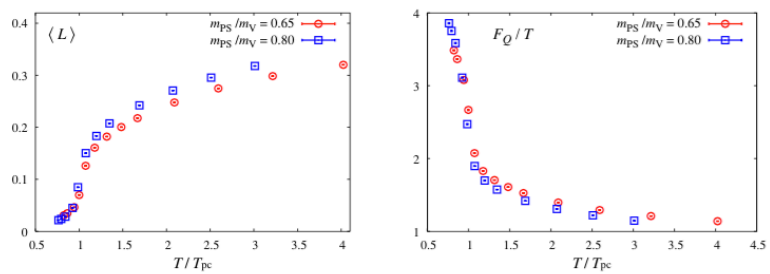

Figure 2.5: Polyakov loop (left) and single-quark free energy (right) on lines of constant physics at $m_{PS}/m_V = 0.65$ (circle) and 0.80 (square) as a function of temperature.

shows the free energy of a single quark defined as

$$\frac{F_Q}{T} = -\ln\langle L\rangle. \tag{2.62}$$

We find that the free energy for smaller quark mass is smaller below T_{pc}, whereas it is larger above T_{pc} than that for larger quark mass. This implies that the anti-screening (screening) properties in the confinement (deconfinement) phase becomes strong when the quark mass is reduced.

The physical meanings of the Polyakov loop can be seen as follows. Consider the equation of motion for the heavy quark field which is written as $e^{-m_Q\tau}\psi$ (upper component of the Dirac spinor). The static Dirac equation for ψ is given as,

$$\left(i\frac{\partial}{\partial\tau} + gA_4(\tau,\mathbf{x})\right)\psi(\tau,\mathbf{x}) = 0. \tag{2.58}$$

The solution is

$$\psi^a(\tau,\mathbf{x}) = \Omega^{ab}(\mathbf{x})\,\psi^b(0,\mathbf{x}), \tag{2.59}$$

where color indices are written explicitly. When the heavy (static) quark is placed at a spatial point $\mathbf{x}$, the partition function (Z_Q) for the single quark can be written by the total Hamiltonian H_Q as:

$$\begin{aligned} Z_Q/Z &= e^{-(F_Q(T,V)-F(T,V))/T} \\ &= \frac{1}{Z}\frac{1}{N_c}\sum_{a=1}^{N_c}\sum_n \langle n|\psi^a(0,\mathbf{x})e^{-H_Q/T}\psi^{\dagger a}(0,\mathbf{x})|n\rangle \\ &= \frac{1}{Z}\frac{1}{N_c}\sum_{a=1}^{N_c}\sum_n \langle n|e^{-H_Q/T}\psi^a(1/T,\mathbf{x})\psi^{\dagger a}(0,\mathbf{x})|n\rangle \\ &= \frac{1}{Z}\frac{1}{N_c}\mathrm{tr}\left[e^{-H/T}\mathrm{tr}\Omega(\mathbf{x})\right] = \langle L(\mathbf{x})\rangle, \end{aligned} \tag{2.60}$$

where F_Q (F) is the free energy with (without) the heavy quark. In the $N_f = 0$ case, the free energy of a single quark can strictly distinguish the confinement phase and the deconfinement phase. Although the Polyakov loop is no longer the order parameter for confinement-deconfinement transition in the case with dynamical quarks, we can utilize the $\langle L\rangle$ as an indicator to separate the cold and hot phases in the parameter space (see Fig. 2.2). The nu-

as the Polyakov loop averaged over all thermal states and spatial points,

$$\langle L\rangle = \frac{1}{Z}\frac{1}{N_s^3}\sum_{\mathbf{x}}\mathrm{Tr}\left[e^{-H/T}L(\mathbf{x})\right]. \tag{2.61}$$

The Polyakov loop has finite values even below T_{pc} because a single heavy quark can exist in the confinement phase due to the dynamical screening from the light quarks. Figure 2.5(right)

Maezawa '07

CUJET3.0 = CUJET2.0 + semi-QGP + mag. monopoles

$$\frac{dE}{dx} \propto \ldots \int_{q^2} \left[\frac{n_e \left(\alpha_s(q^2)\alpha_s(q^2)\right) f_E^2}{q^2(q^2+f_E^2\mu^2)} + \frac{n_m \left(\alpha_s^e(q^2)\alpha^m(q^2)\right) f_M^2}{q^2(q^2+f_M^2\mu^2)} \right] \ldots$$

$$\frac{dE}{dx} \propto \ldots \int_{q^2} \frac{n_e\, \alpha_s^2(q^2)\, f_E^2}{q^2(q^2+f_E^2\mu^2)} \ldots$$

$$\frac{dE}{dx} \propto \ldots \int_{q^2} \frac{n_T}{(q^2+f_E^2\mu^2)(q^2+f_M^2\mu^2)} \times \kappa(q^2,T)$$

$$\kappa(q^2,T) \equiv \alpha_s^2(q^2)\,\chi_T \left(f_E^2 + \frac{f_E^2 f_M^2 \mu^2}{q^2}\right) + (1-\chi_T)\left(f_M^2 + \frac{f_E^2 f_M^2 \mu^2}{q^2}\right)$$

$$\chi_T = c_q\, L + c_g\, L^2 \qquad L(\mathbf{x}) = \frac{1}{N_c}\mathrm{tr}\mathcal{P}\exp\left[ig\int_0^{1/T} A_4(\tau,\mathbf{x})d\tau\right]$$

$$f_E = \sqrt{\chi_T}$$

$$f_M = C_m\, g_T$$

$$x_E \frac{dN_g^{n=1}}{dx_E} = \frac{18C_R}{\pi^2}\frac{4+N_f}{16+9N_f}\int d\tau\, n(\mathbf{z})\Gamma(\mathbf{z}) \int d^2k$$
$$\times\, \alpha_s\left(\frac{\mathbf{k}^2}{x_+(1-x_+)}\right) \int d^2q \frac{\alpha_s^2(\mathbf{q}^2)}{\mu^2(\mathbf{z})} \frac{f_E^2\mu^2(\mathbf{z})}{\mathbf{q}^2(\mathbf{q}^2+f_E^2\mu^2(\mathbf{z}))}$$
$$\times\, \frac{-2(\mathbf{k}-\mathbf{q})}{(\mathbf{k}-\mathbf{q})^2+\chi^2(\mathbf{z})}\left[\frac{\mathbf{k}}{\mathbf{k}^2+\chi^2(\mathbf{z})} - \frac{(\mathbf{k}-\mathbf{q})}{(\mathbf{k}-\mathbf{q})^2+\chi^2(\mathbf{z})}\right]$$
$$\times\left[1-\cos\left(\frac{(\mathbf{k}-\mathbf{q})^2+\chi^2(\mathbf{z})}{2x_+E}\tau\right)\right]\left(\frac{x_E}{x_+}\right)\left|\frac{dx_+}{dx_E}\right| \qquad (1)$$

$$\Gamma(\mathbf{z}) = u_f^\mu n_\mu \qquad n = (1,\vec{\beta}_{jet})$$
$$u_f^\mu = \gamma_f(1,\vec{\beta}_f)$$

Liu et al. 07'; Baier et al. 07'

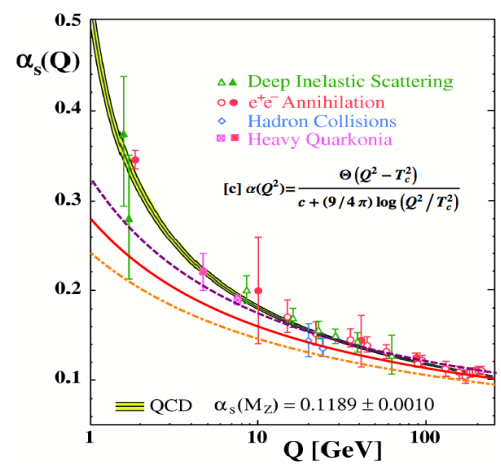

$$\alpha_s^2(q^2) \approx [1/[c + (9/2\pi)Log(q/\Lambda)]]^2$$

Pressure/Entropy Counting & eta/s

- The eta/s in kinetic theory
- Extra factors come from quantum statistics which differ slightly from the Stefan-Boltzmann
- Different counting schemes bring theoretical uncertainties

$$\rho(\mathbf{x}) = \sum \frac{\zeta(3)}{\pi^2} g_i \eta_i T^3(\mathbf{x})$$
$$\epsilon(\mathbf{x}) = \sum \frac{\pi^2}{30} g_i \eta_i' T^4(\mathbf{x})$$
$$p(\mathbf{x}) = \epsilon(\mathbf{x})/3$$
$$s(\mathbf{x}) = \frac{p(\mathbf{x}) + \epsilon(\mathbf{x})}{T} \approx \kappa \rho(\mathbf{x})$$

$$\frac{\eta}{s} = \frac{18}{5} \frac{T^3}{s(T)} \sum_a \frac{d_a(T)}{\sum_b d_b(T) F_{ab}(T)}$$

$$a, b = q, g, m$$
$$d_q = c_q \cdot L(T)\ (PR)\ or\ c_q \cdot L(T)/N_s\ (SR)$$
$$d_g = c_g \cdot L^2(T)\ (PR)\ or\ c_g \cdot L^2(T)/N_s\ (SR)$$
$$d_m = 1 - d_q - d_g$$

$$F_{ab}(T) = \int_0^{9T^2} dq^2 \frac{2\pi q^2 C_{ab} \alpha_a \alpha_b}{(q^2 + f_E^2 \mu^2)(q^2 + f_M^2 \mu^2)}$$

$$\alpha_q = \alpha_g = \alpha_E\ ,\ \alpha_m = 1/\alpha_E$$
$$C_{qq} = 4/9$$
$$C_{qg} = C_{gq} = C_{qm} = C_{mq} = 1$$
$$C_{gg} = C_{mm} = 9/4$$

Fast Liberation Scheme (FL)

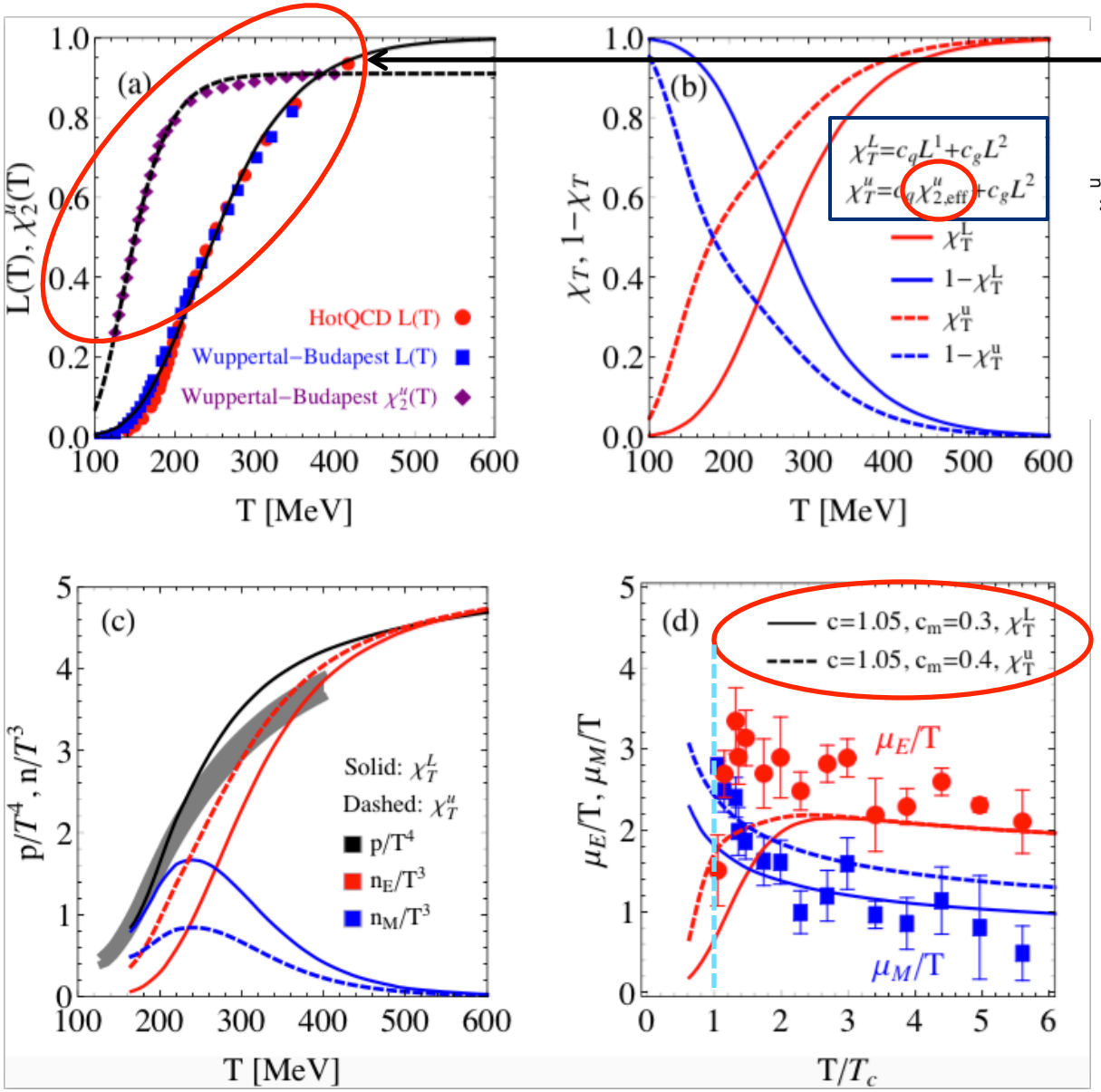

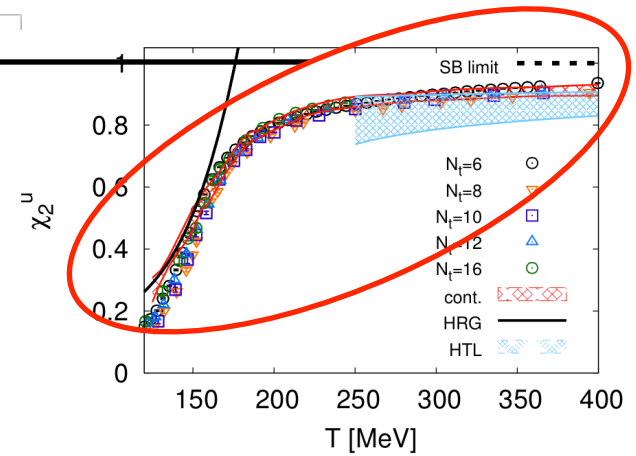

Wuppertal-Budapest JHEP 1201 (2012) 138

- Fast Quark Liberation: Fit to lattice QCD u quark number susceptibility
- Note the shift of E&M fractions and screening masses near Tc

$$\frac{p}{T^4} = \frac{1}{VT^3} \ln Z(V, T, \mu_B, \mu_S, \mu_Q)$$

$$\chi_{lmn}^{BSQ} = \frac{\partial^{l+m+n} p/T^4}{\partial(\mu_B/T)^l \partial(\mu_S/T)^m \partial(\mu_Q/T)^n}.$$

$$\chi_2^X = \frac{1}{VT^3} \langle N_X^2 \rangle$$

CUJET3.0: RAA & v2 at RHIC & LHC in FL

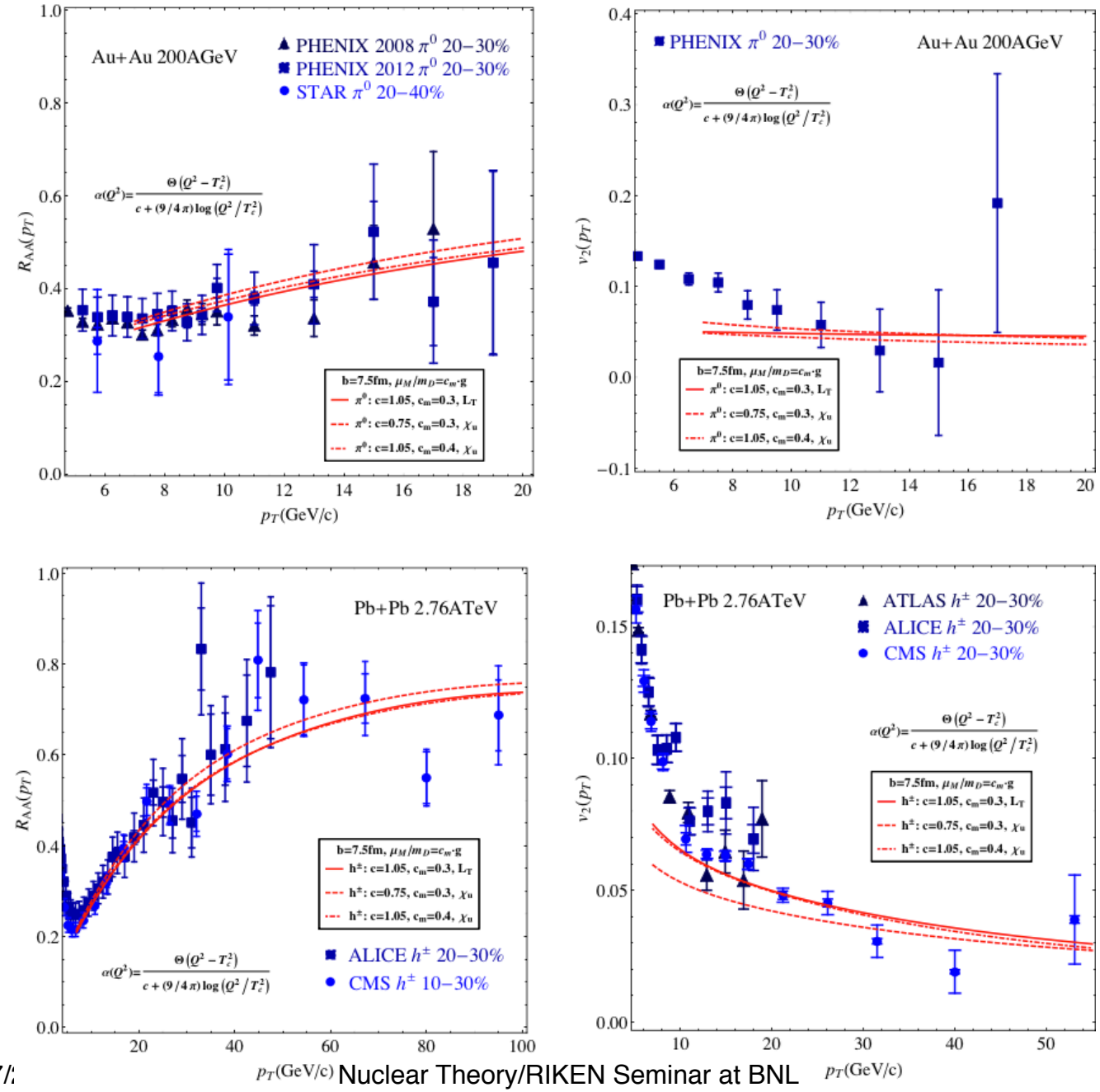

CUJET3.0: RAA & v2 at RHIC & LHC in FL

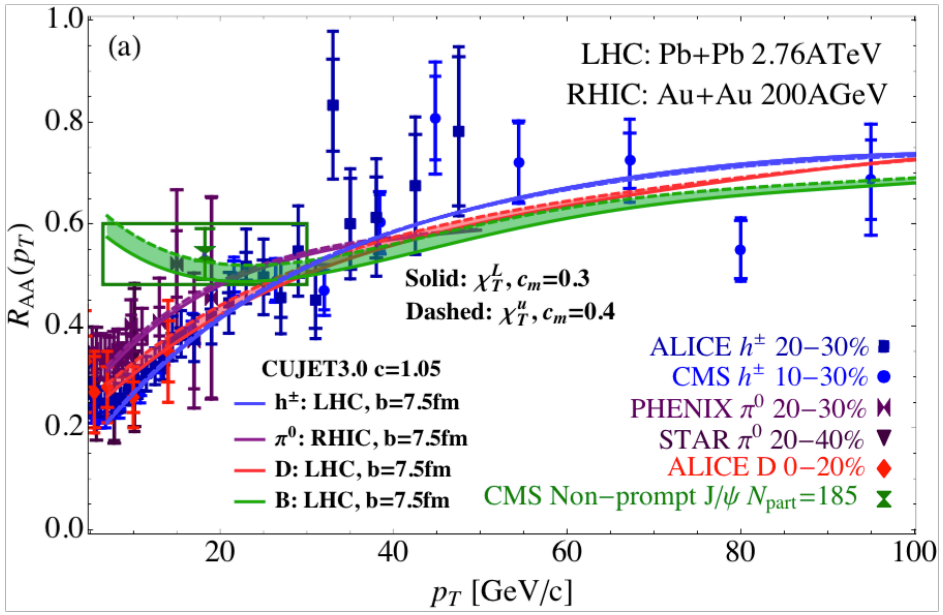

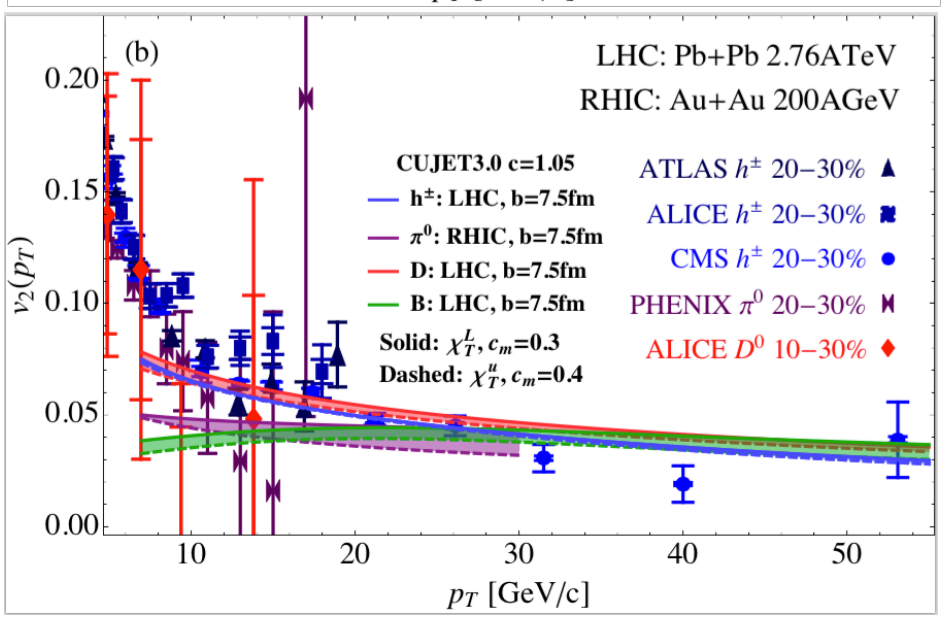

- In the fast liberation scheme, the CUJET3.0 model with $(c,c_m)=(1.05,0.4)$ fits both R_{AA} and v_2 at both RHIC and LHC

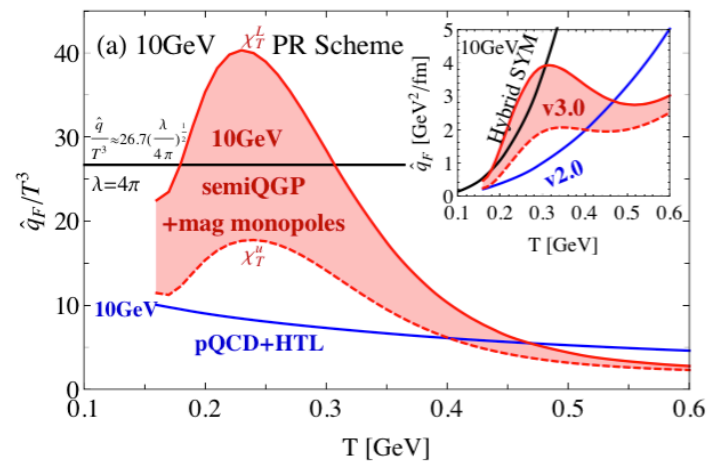

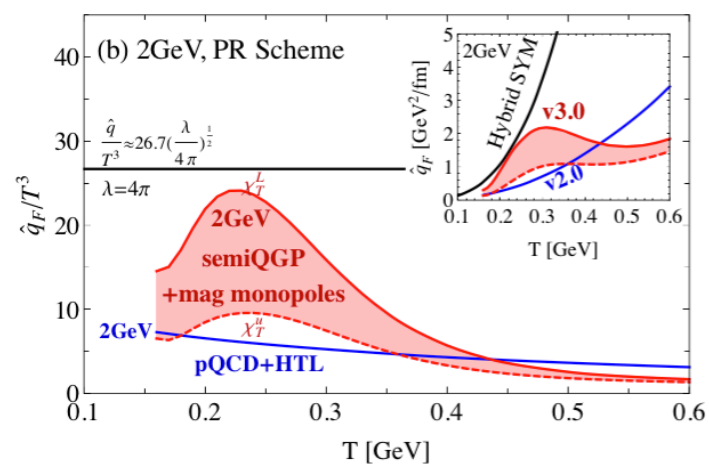

CUJET3.0: eta/s in the fast liberation scheme

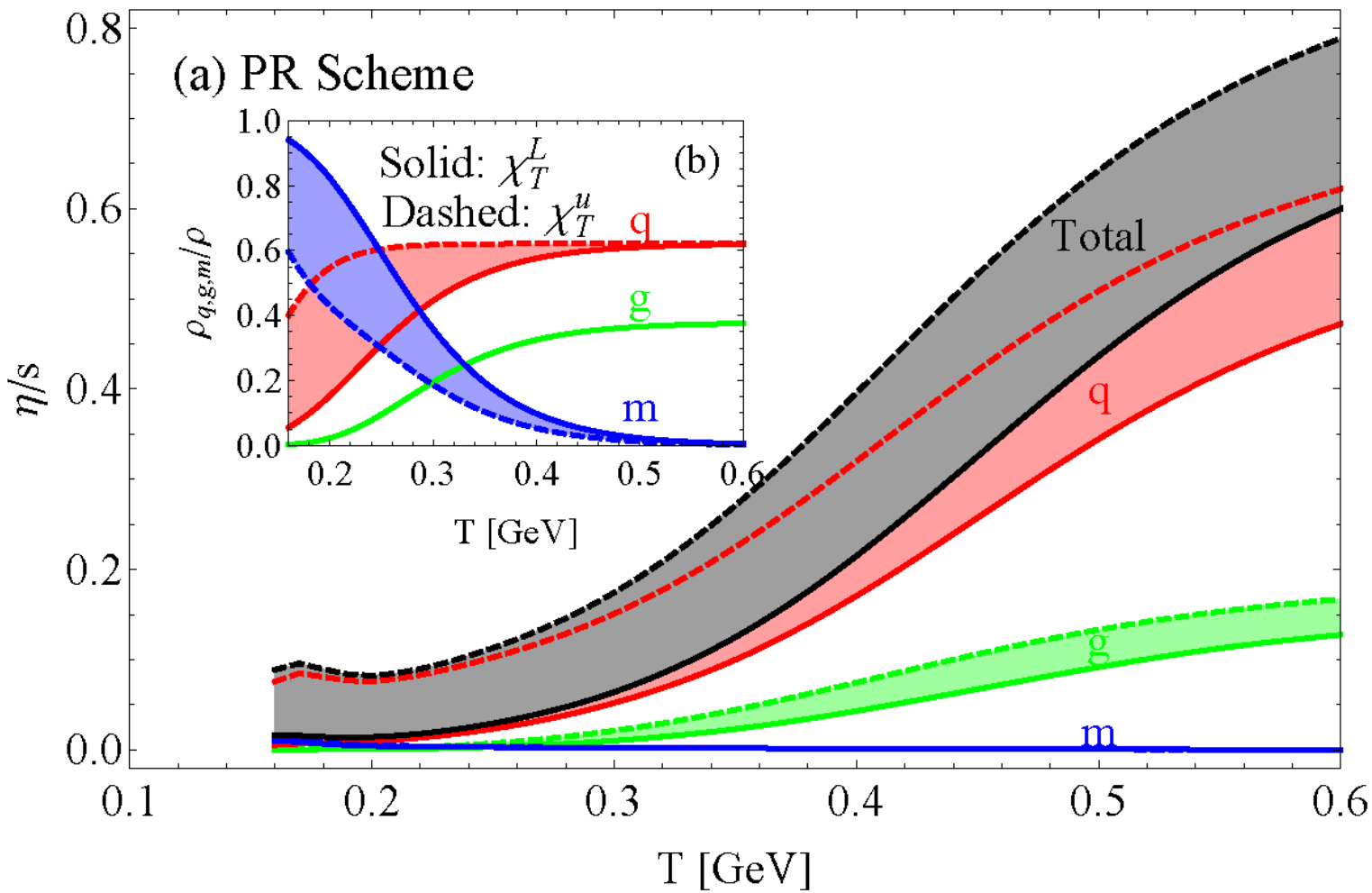

❖ Fast liberation gives a better eta/s near Tc

HTL vs semi vs anti-semi vs CUJET3.0

- HTL: amax=0.26
- semi: amax=0.44
- anti-semi: amax=0.36
- CUJET3.0: c=1.05

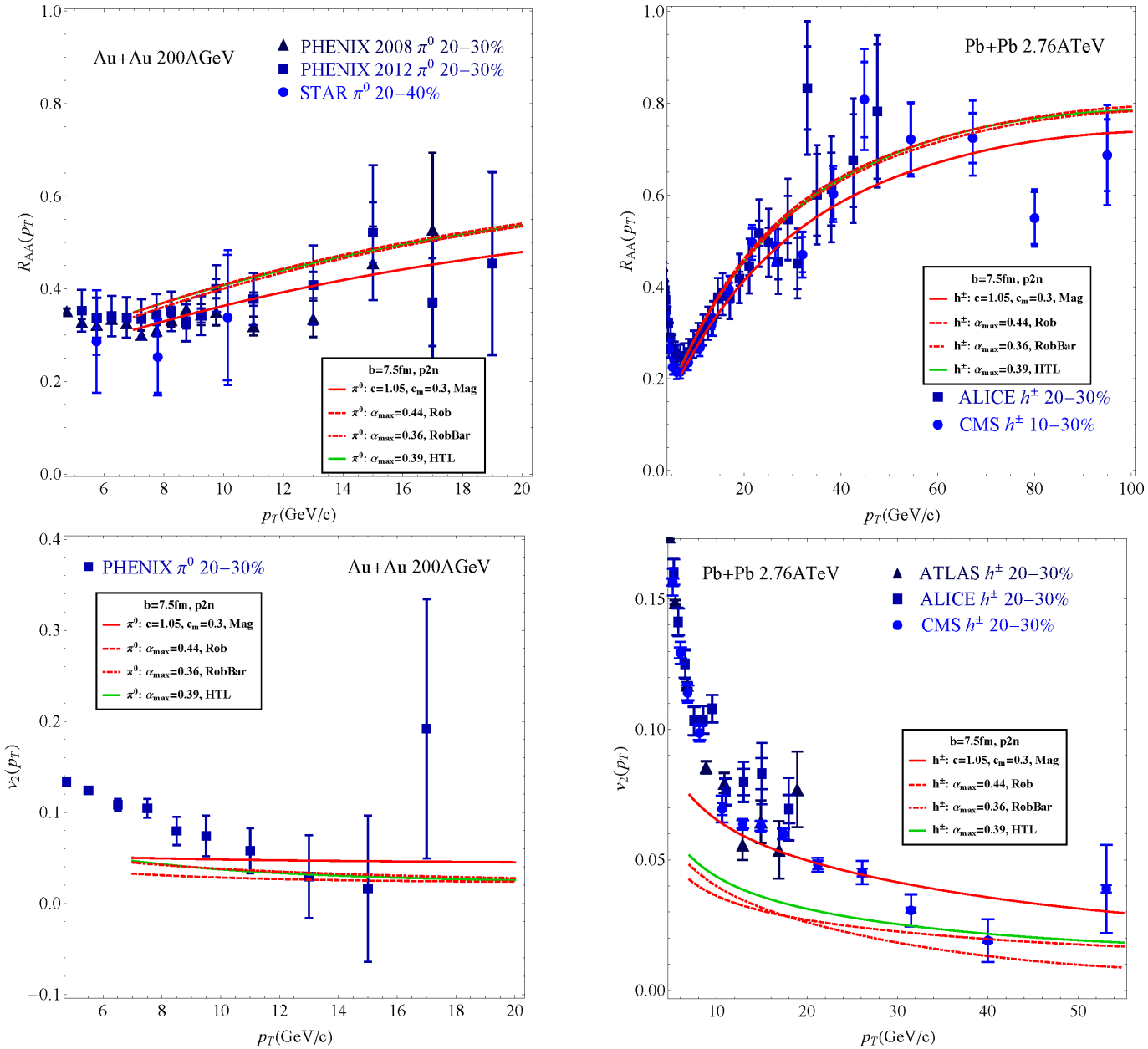

HTL vs semi vs anti-semi vs CUJET3.0

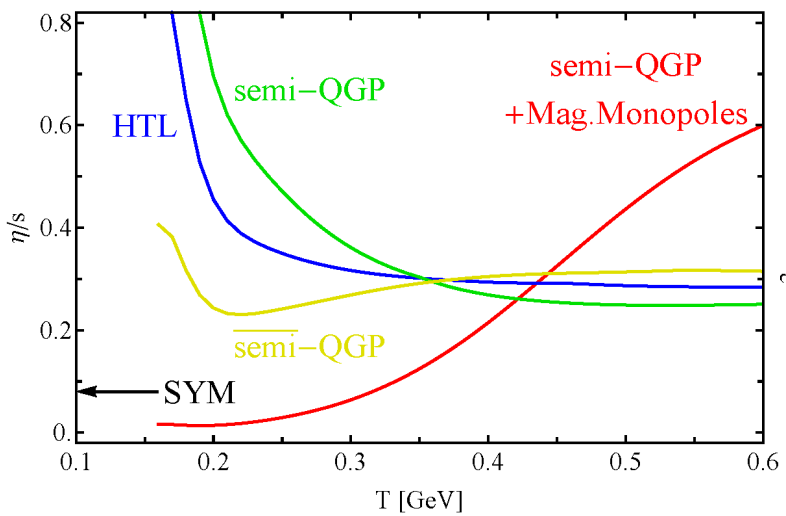

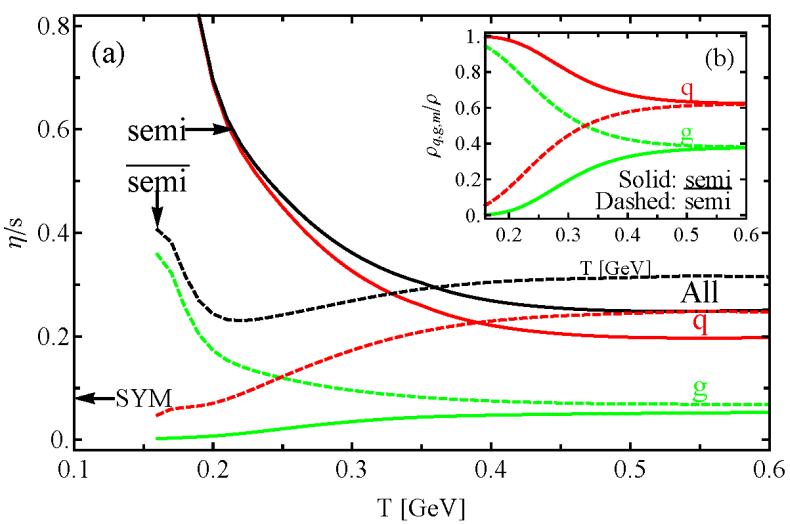

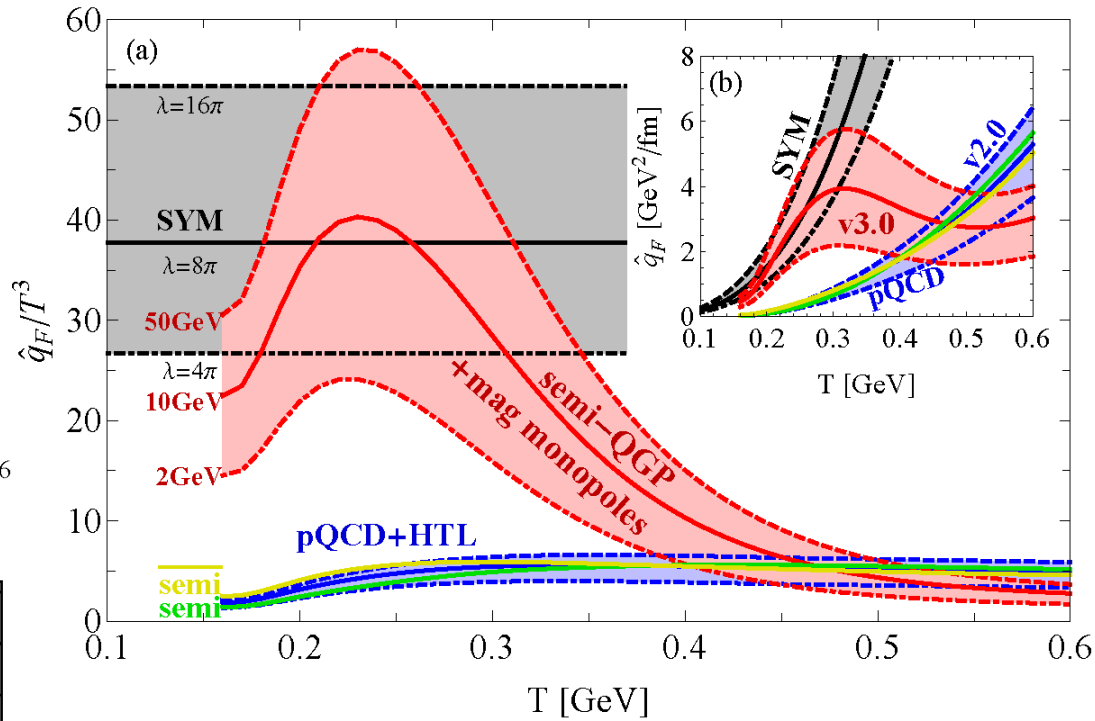

- Both “semi” and “anti-semi”’s qhat deviate negligibly from the pQCD+HTL limit
- Semi-QGP along cannot account for the perfect fluidity near Tc
- “semi”: amax=0.44; “anti-semi”:amax=0.36

Relativistic corrections to jet quenching from transverse flow

$$\Gamma(\mathbf{z}) = u_f^\mu n_\mu \quad n = (1, \vec{\beta}_{jet}) \quad u_f^\mu = \gamma_f (1, \vec{\beta}_f)$$

Liu et al. 07'; Baier et al. 07'

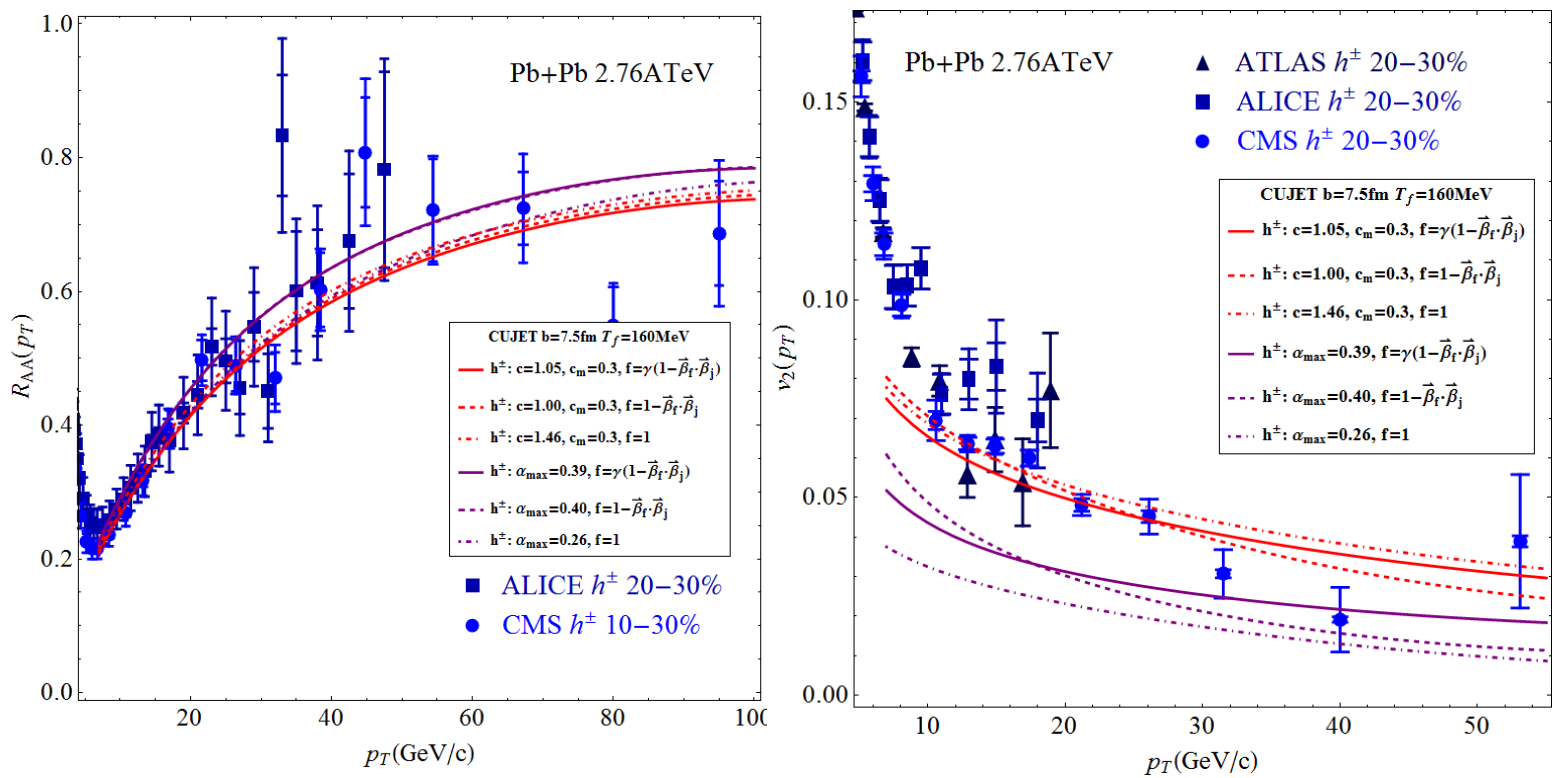

- Both RAA and v2 are surprisingly insensitive to the form of the relativistic flow corrections in both CUJET2.0 (pQCD+HTL) and CUJET3.0 (semi-QGP + magnetic monopoles)

CUJETv3.0 vs v2.0: the path length dependence of energy loss

log(ΔE/E) vs log(L)

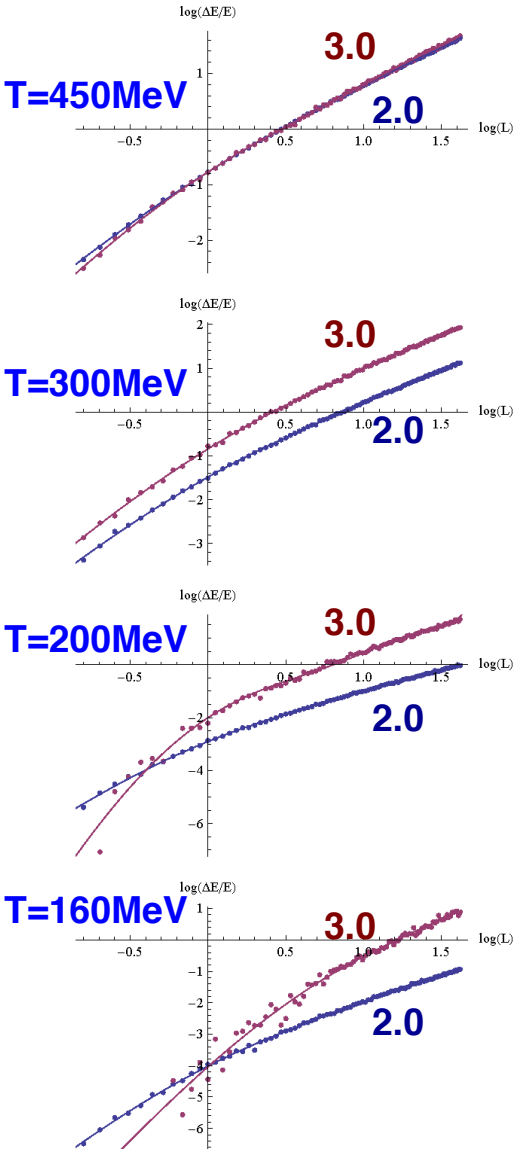

n(L) vs L; dE/dL~L^n

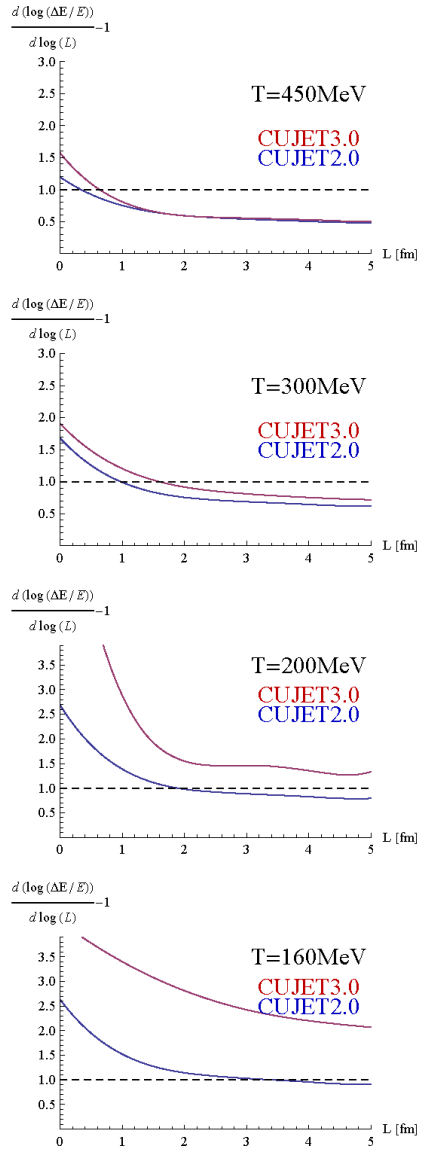

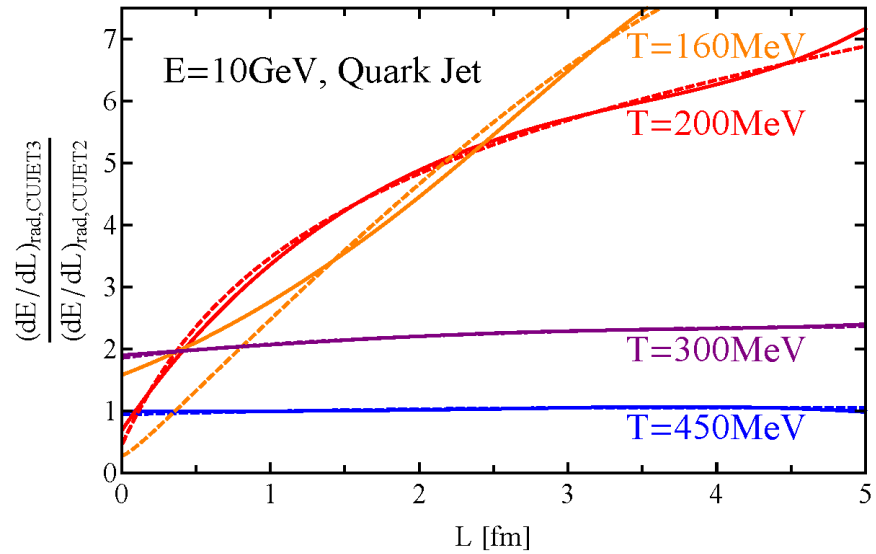

- At high T, v2.0 and v3.0 are similar, both bearing dE/dL~L^n with n~0.5, stronger than linear and weaker than quadratic
- At intermediate T, v2.0 and v3.0 are approximately similar with n~1
- At near-Tc temperatures, CUJET v2.0 is roughly a quadratic dependence and v3.0 is about CUBIC!
  - At small distances, the energy loss of v3.0 is smaller than v2.0=pQCD+HTL